Preconditioners for monolitic multi-physics problems – with applications toward the biomechanics of the brain

Kent-Andre Mardal

University of Oslo /

Simula Research Laboratory

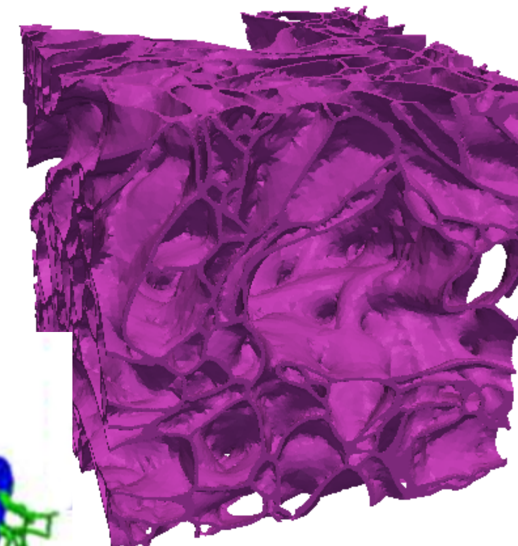

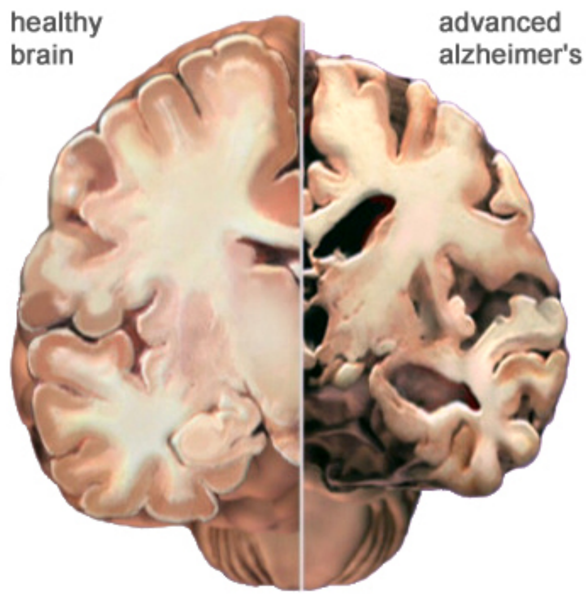

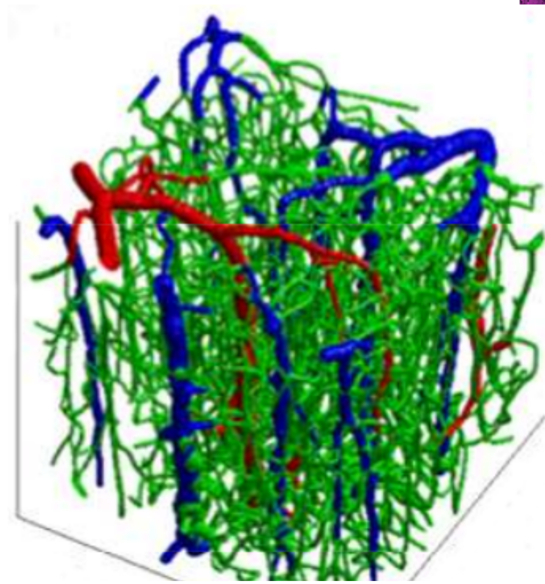

MWNDEA 2020

Monash Workshop on Numerical Differential Equations and Applications 2020

Outline

- Alzheimer´s disease & the glymphatic system
- Modeling of the glymphatics and brain mechanics: controversies, previous attempts
- Preconditioning of multi-physics / multi-scale models

The greying of Europe

- Cost of Alzheimer´s disease in Europe amounts to about 1% of GDP and will increase
- The disease develops over decades and early treatment has significant potential
- Little effort spent by the computational or biomechanics community compared to sophisticated models that have been developed for cardiovascular diseases
- The hallmark feature of the disease is accumulation of metabolic waste (amyloid beta) (as is also common for other types of dementia)

Overview of the poro-elastic brain

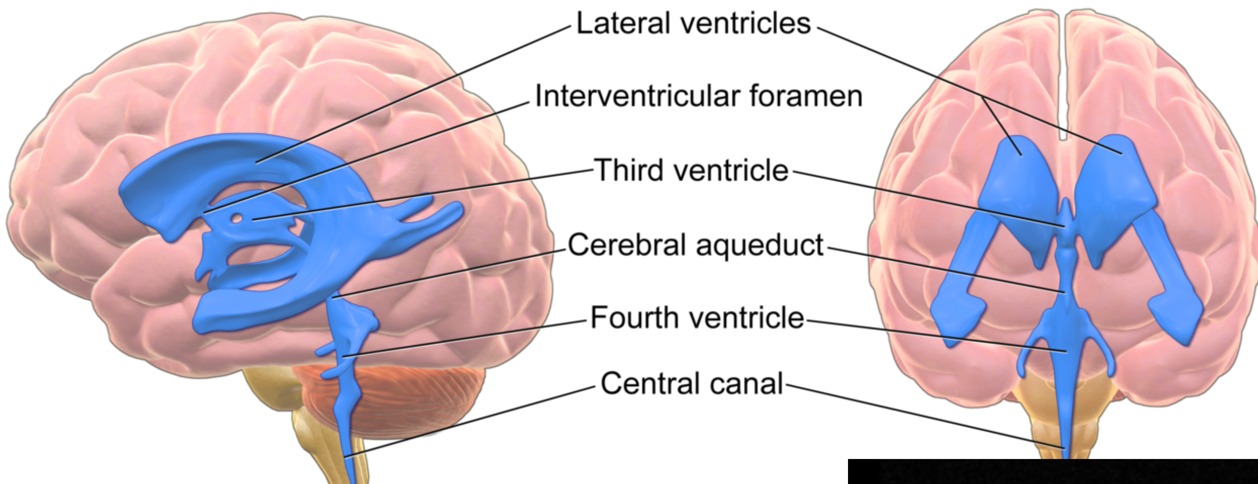

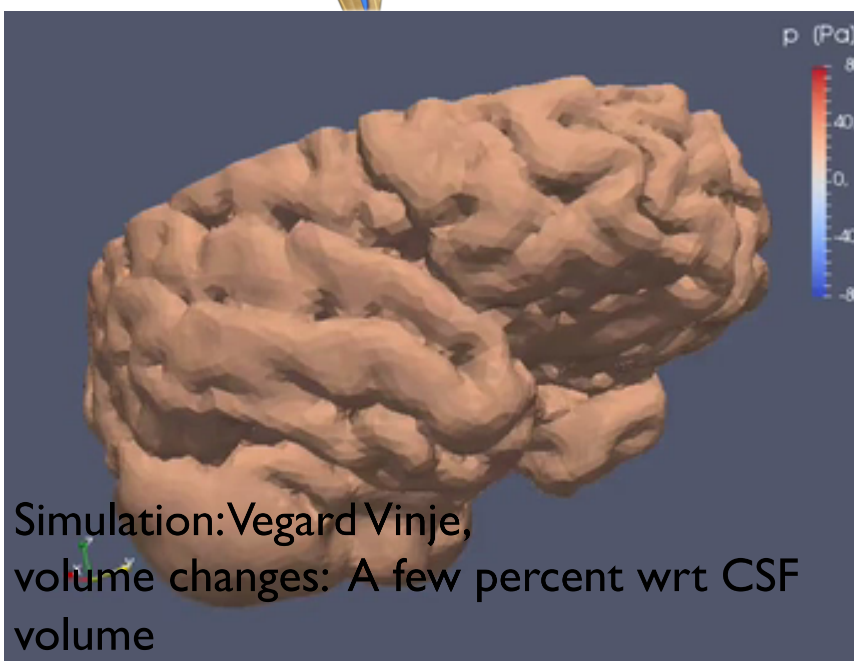

Simulation: Vegard Vinje,
volume changes: A few percent wrt CSF volume

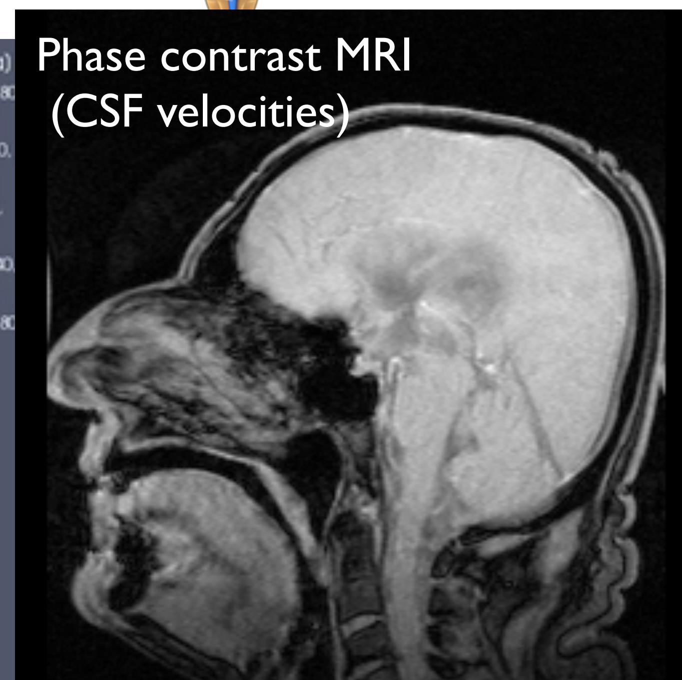

Phase contrast MRI
(CSF velocities)

Basic facts about the brain's metabolism

- The brain occupies 1-2% of the body in volume / weight
- The brain consumes around 10-20% of the body's energy, oxygen
- Elsewhere in the body, the lymphatic system plays a central role in the disposal of waste
- The brain does not have a lymph system and how the brain clears waste is currently unknown
- Comment: The brain is special because it is bathed in water (cerebrospinal fluid).

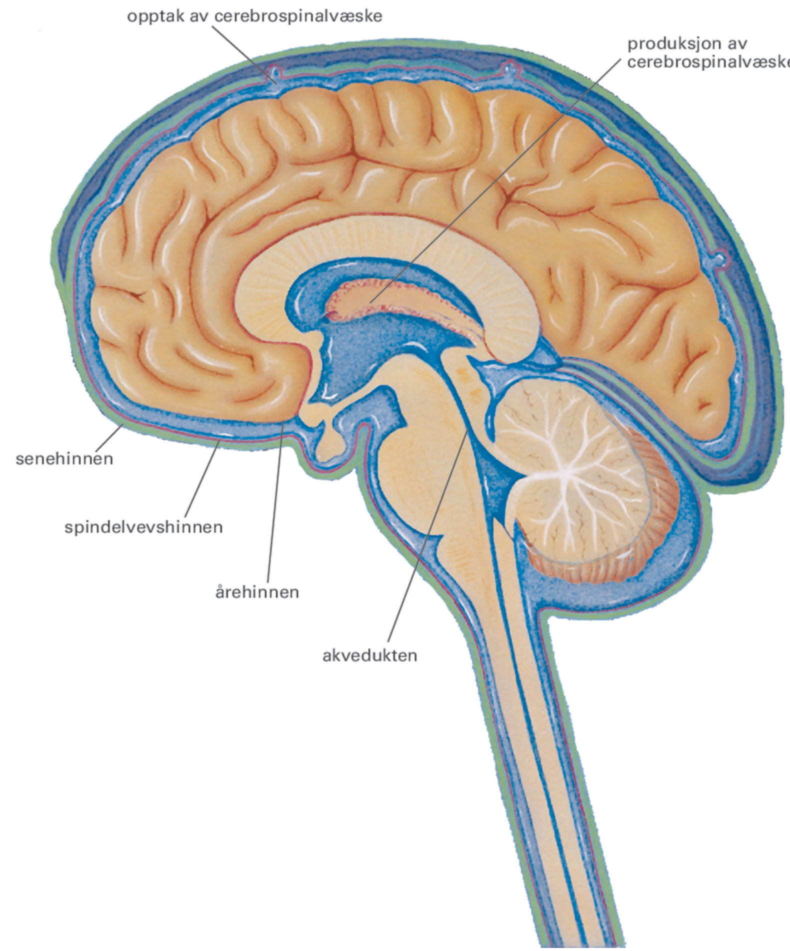

Glymphatic system: the garbage truck of the brain

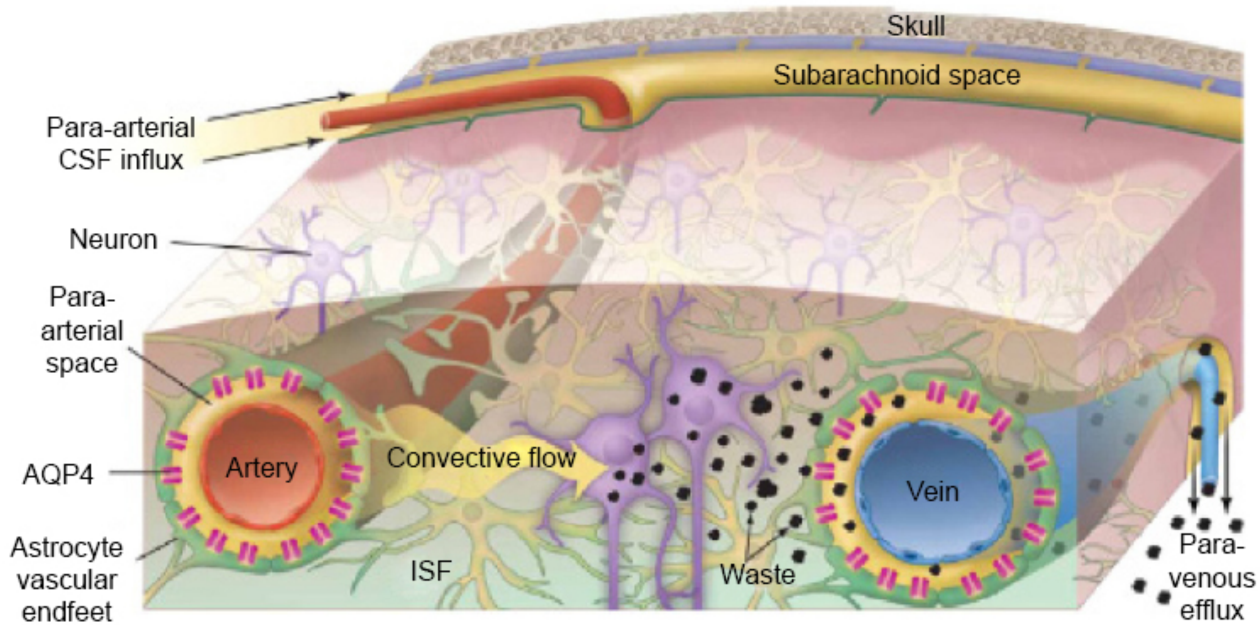

The new pathway:

- the paravascular space that surrounds the arteries/arterioles are connected with the CSF that surrounds the brain. This space facilitate a bulk flow (viscous flow)
- the hydrostatic pressure gradient between the arterial and venous sites facilitate a bulk flow through the interstitium (porous flow)
- the waste is then removed on the venous site (viscous flow)

Nedergaard M. Garbage truck of the brain. Science. 2013

The glymphatic system is hyperactive during sleep because the extracellular volume increases

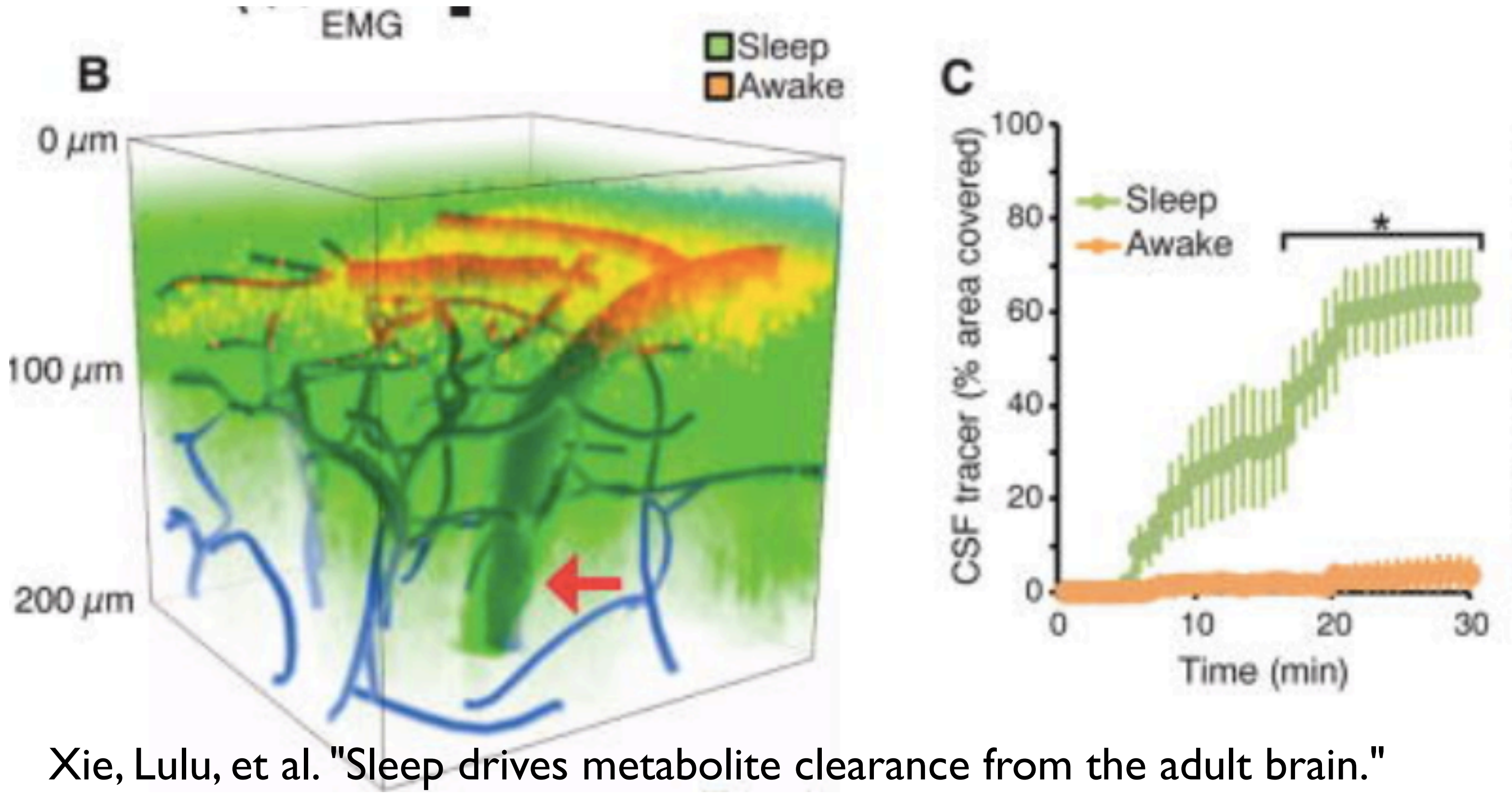

Xie, Lulu, et al. "Sleep drives metabolite clearance from the adult brain." Science 2013

3 kDa Texas Red Dextran typically penetrated 100-200 µm in about 20 minutes

Characteristics of Alzheimer´s disease from a modeling point of view

- Massive brain shrinkage
- Accumulation of waste (amyloid beta) leading to cell death
- The accumulation of waste suggests that the glymphatic system is malfunctioning
- Hence, a proper understanding of this system may have significant potential

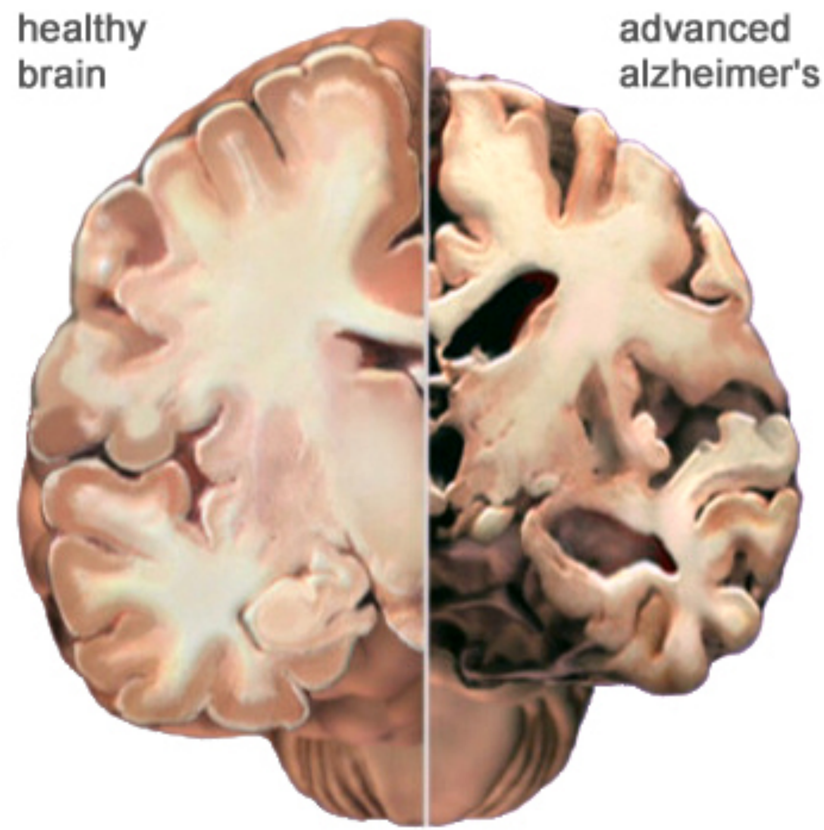

Extracellular flow driven by a hydrostatic gradient: What is the effective permeability, flow and pressure?

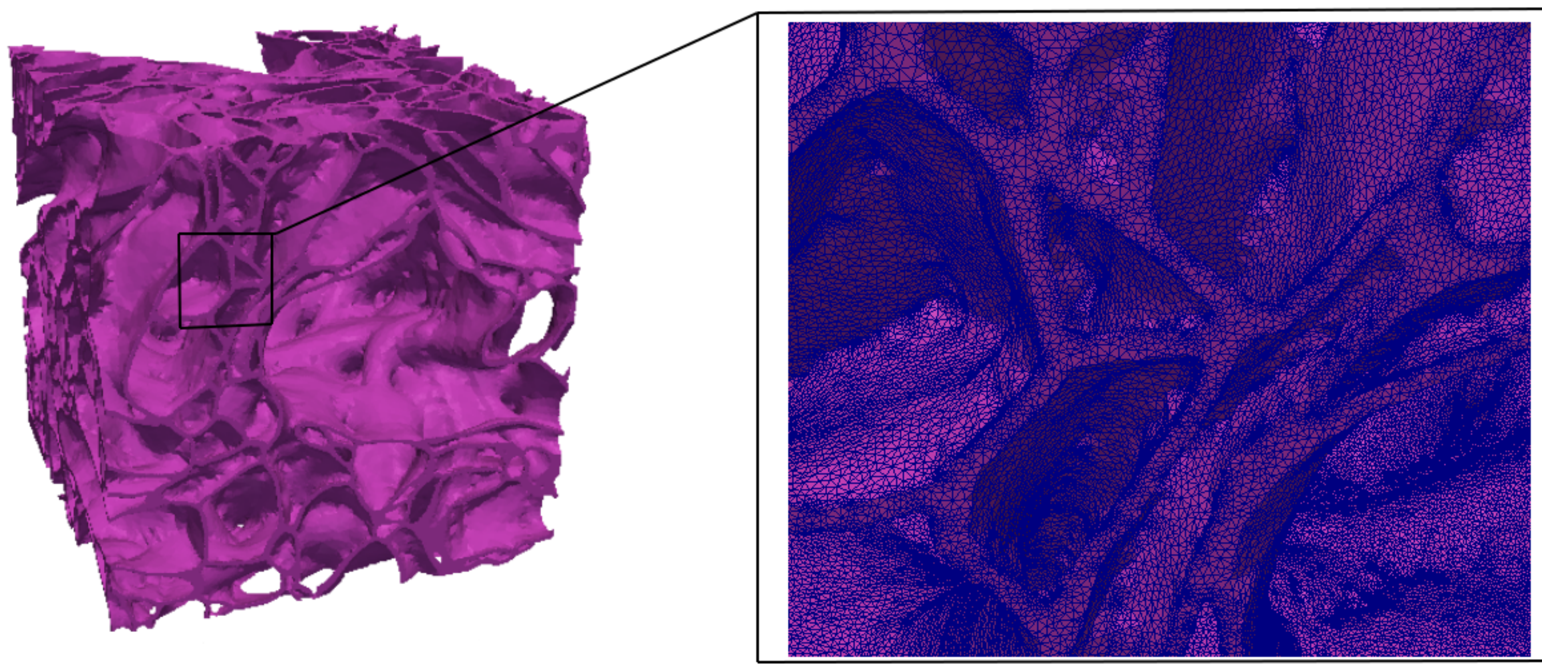

Piece of grey matter from rat, ~(5 micron)^3
Meshes 54-84 M cells
Extracellular space 10-20%
Pressure drop: 1 mmHg / mm
Stokes flow simulations: ~ 500 CPU hours / 3 hours real-time

Kinney et.al , J of comparative neurology, 2013

Velocities are 100 times slower, permeability also 100 times smaller than expected, and diffusion dominates:

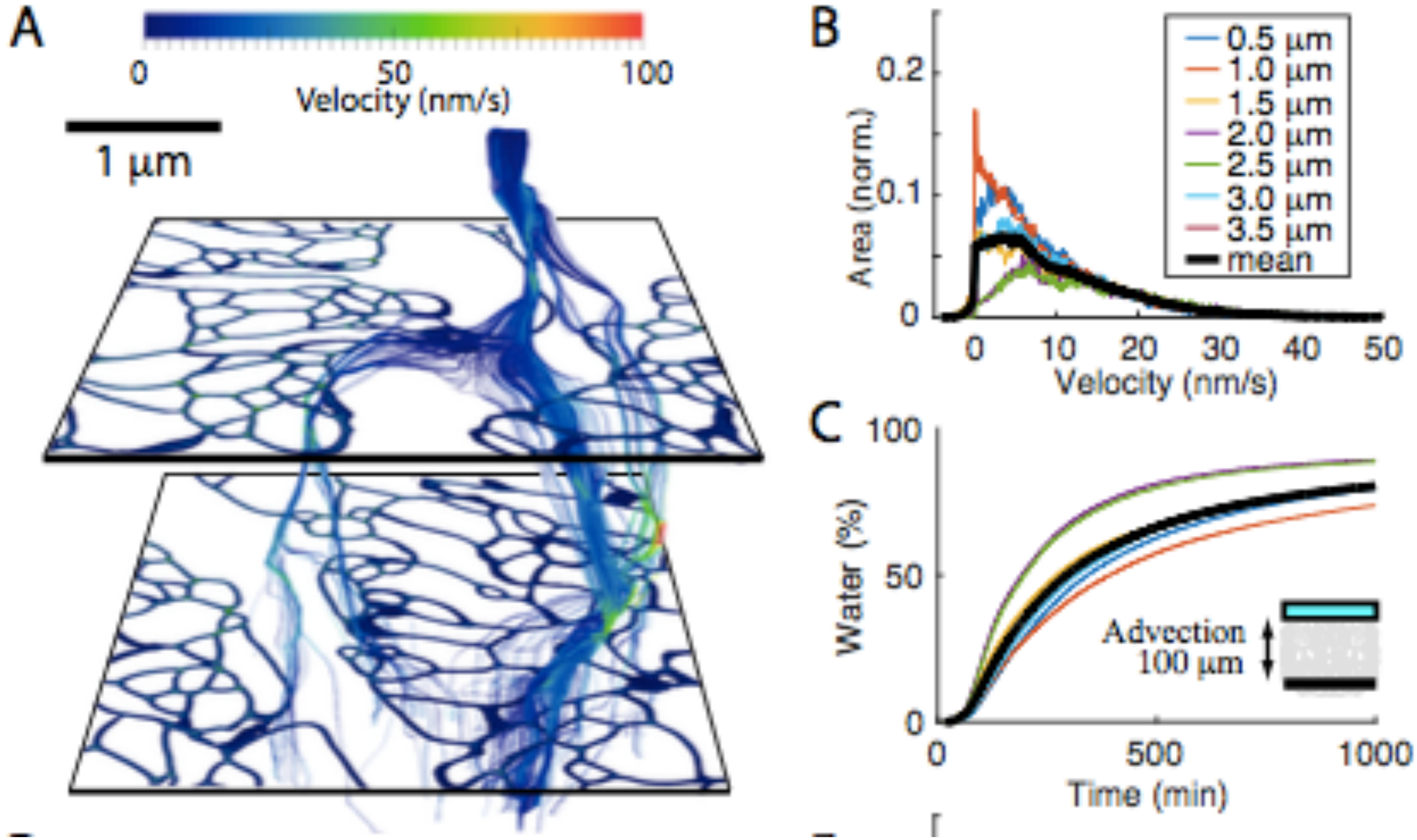

Computational models suggest no bulk flow: diffusion dominates in the interstitium – the porous flow is too slow

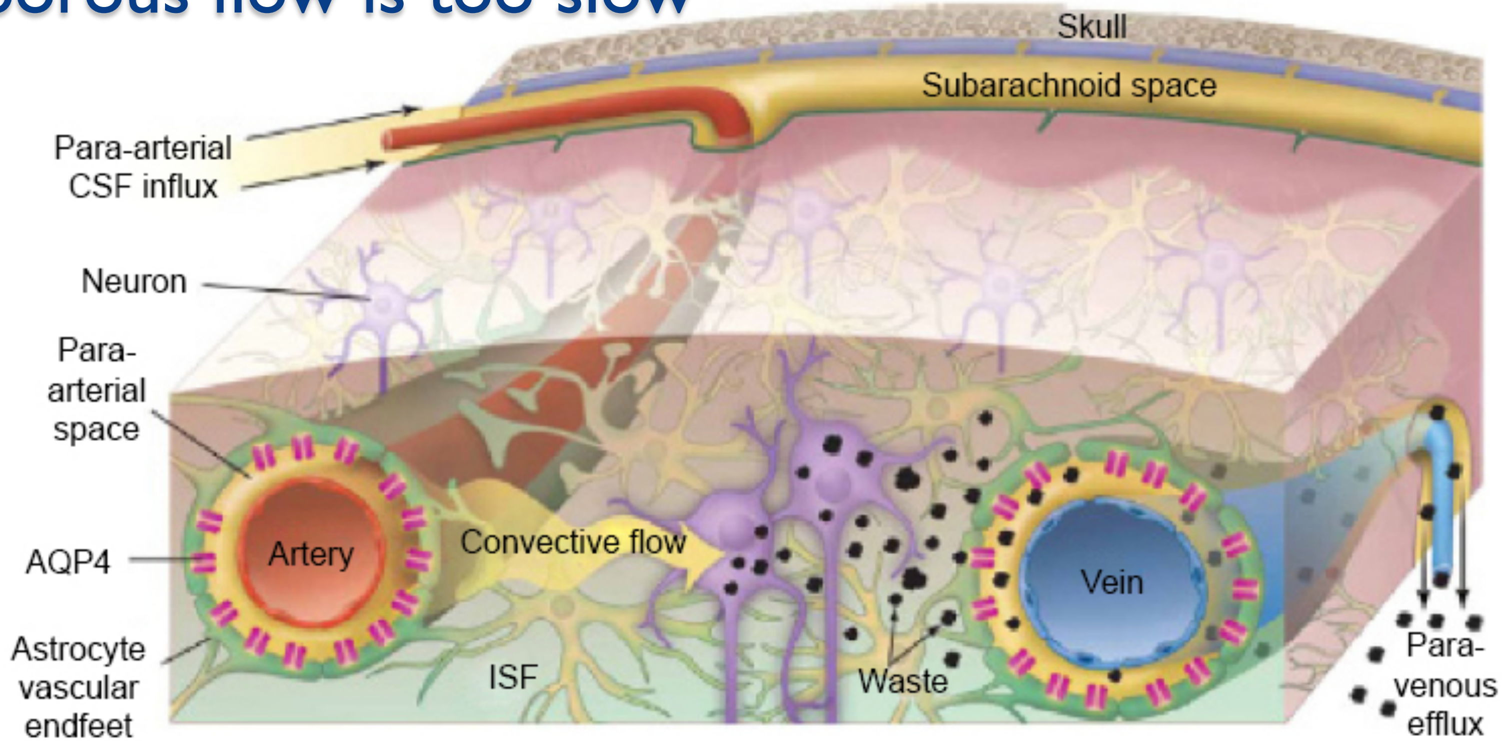

Jin BJ, Smith AJ, Verkman AS. Spatial model of convective solute transport in brain extracellular space does not support a "glymphatic" mechanism. The Journal of general physiology. 2016

Holter KE, Kehlet B, Devor A, Sejnowski TJ, Dale AM, Omholt SW, Ottersen OP, Nagelhus EA, Mardal KA, Pettersen KH. Interstitial solute transport in 3D reconstructed neuropil occurs by diffusion rather than bulk flow. Proceedings of the National Academy of Sciences. 2017

Glymphatic system: the garbage truck of the brain – the viscous flow is to slow …

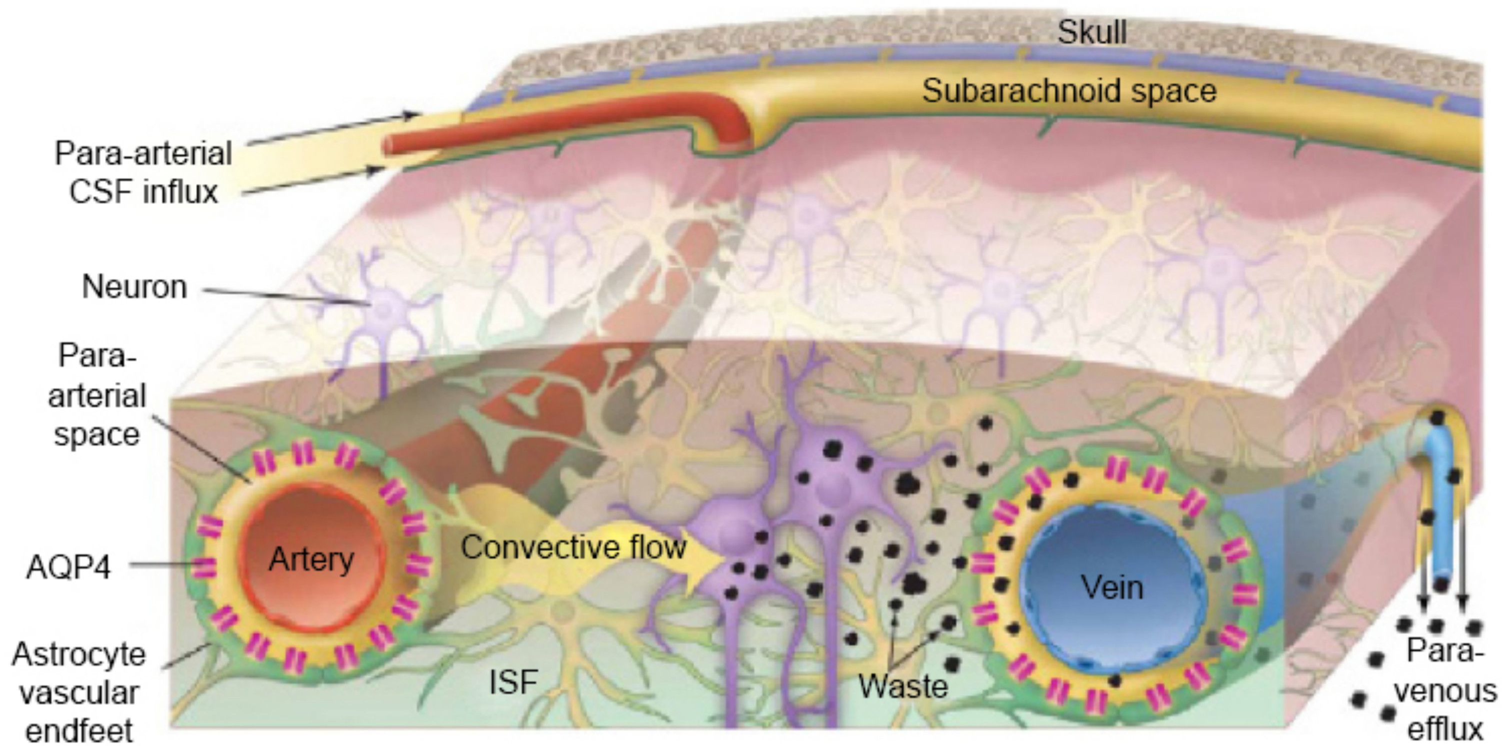

M. K. Sharp, R. Carare, and B. Martin, "Dispersion in porous media in oscillatory flow between flat plates: Ap- plications to intrathecal, periarterial and paraarterial solute transport in the central nervous system," Journal of Fluid Mechanics, Accepted

M. Asgari, D. De Zelicourt, and V. Kurtcuoglu, "Glymphatic solute transport does not require bulk flow," Scientific reports, vol. 6, 2016.

Both papers find that because the peria/para vascular spaces are narrow; bulk flow or dissipation effects will be small

Glymphatic system: the garbage truck of the brain

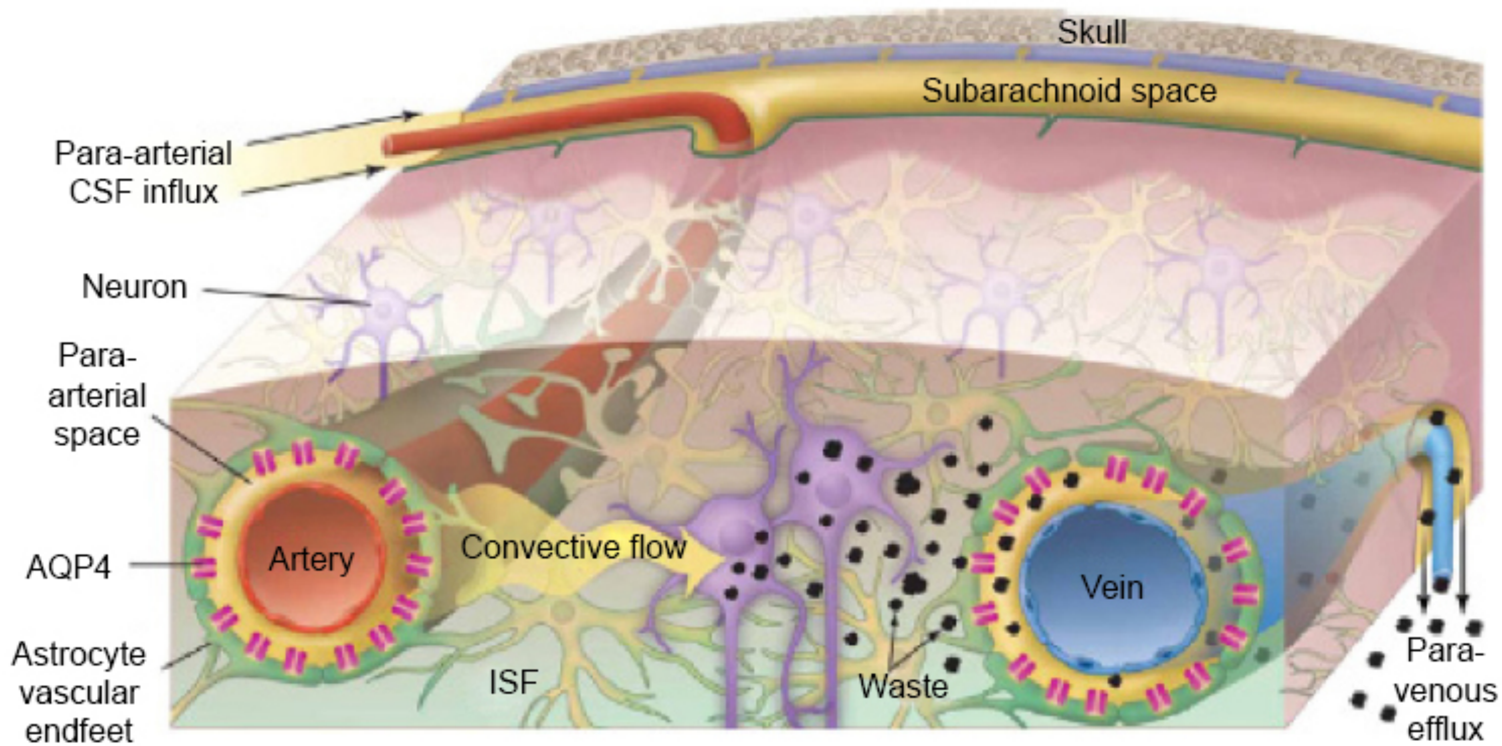

The new pathway:

- the paravascular space that surrounds the arteries/arterioles are connected with the CSF that surrounds the brain. This space facilitate a bulk flow
- the hydrostatic pressure gradient between the arterial and venous sites facilitate a bulk flow through the interstitium
- the waste is then removed on the venous site

New MRI investigations

Intrathecal MR-contrast

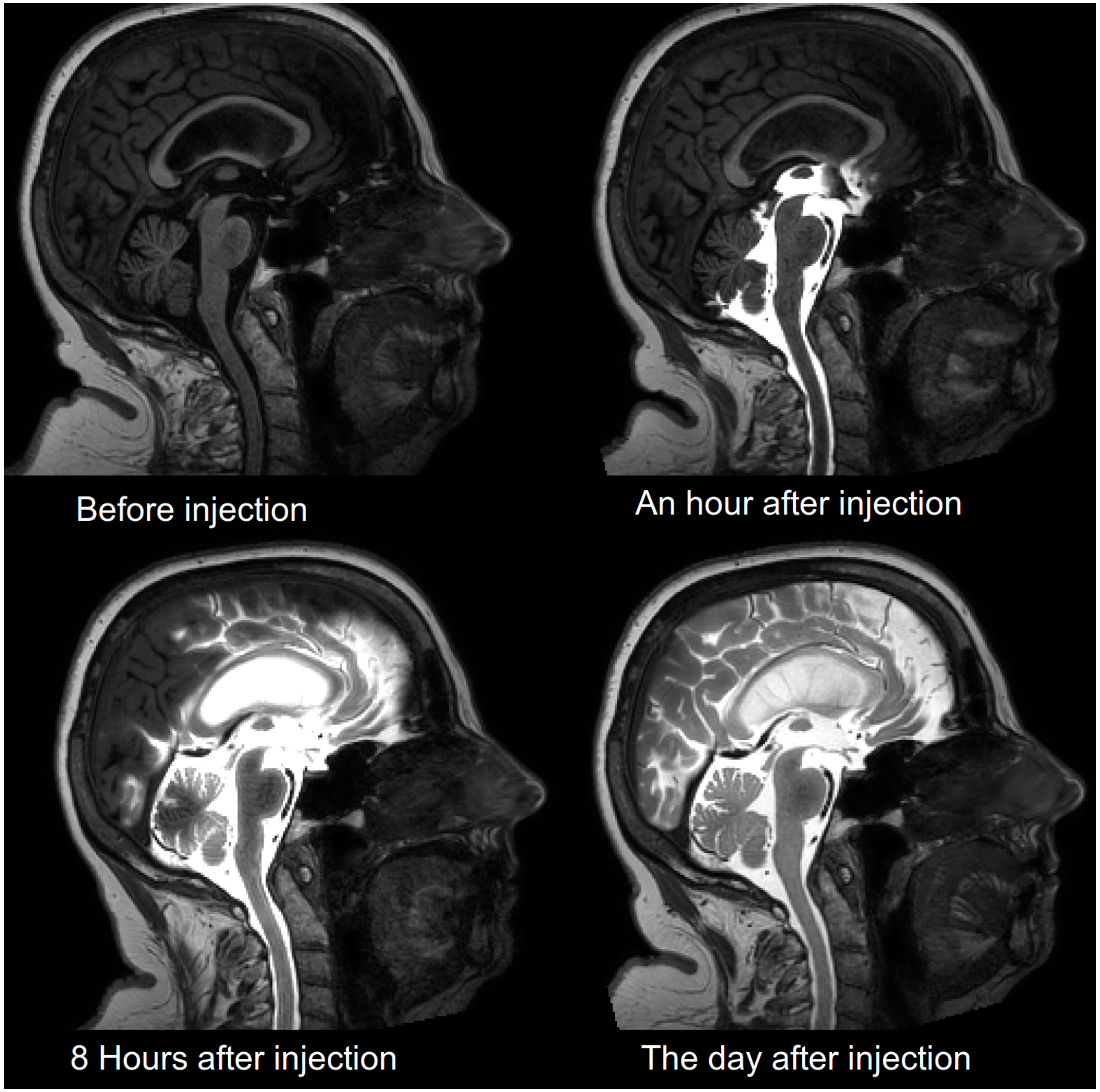

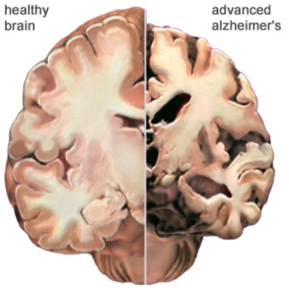

With Lars Magnus Valnes, Geir Ringstad, Per Kristian Eide

Intrathecal MR-contrast

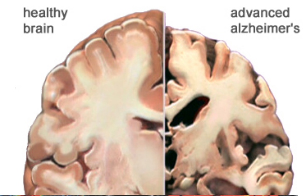

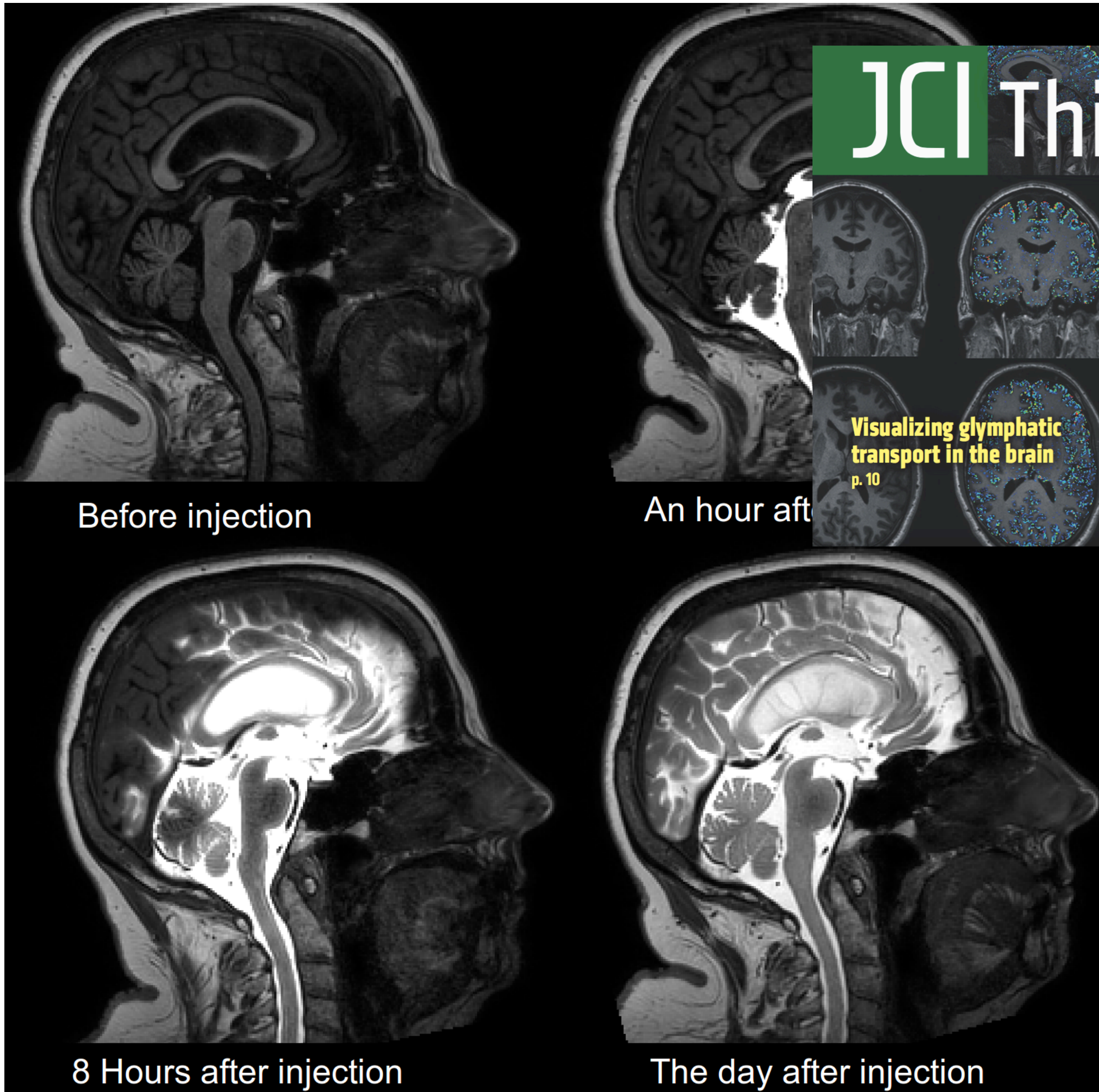

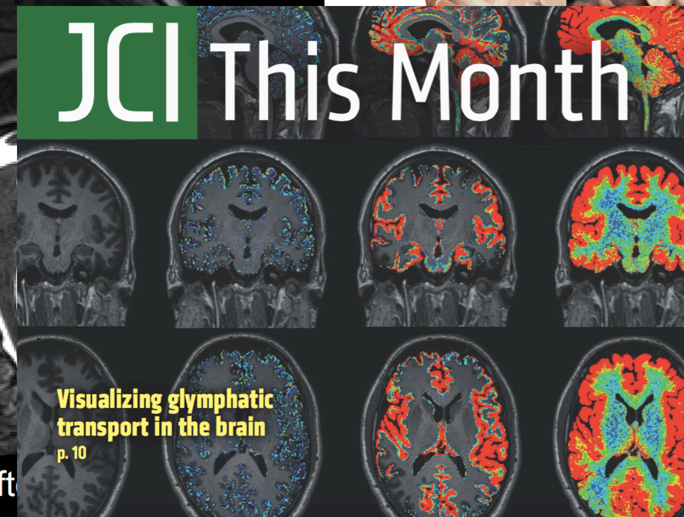

With Lars Magnus Valnes, Geir Ringstad, Per Kristian Eide

Intrathecal MR-contrast

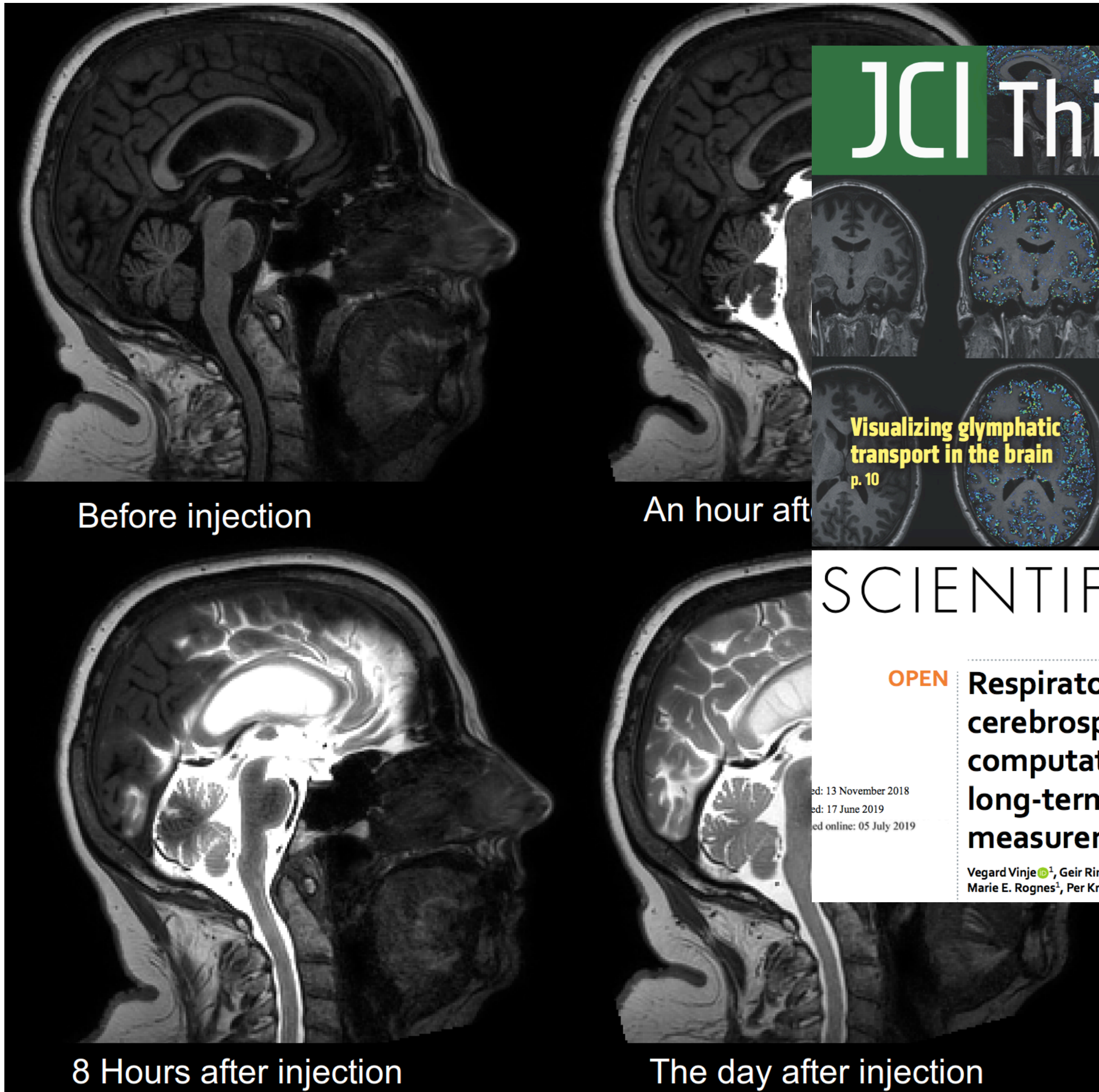

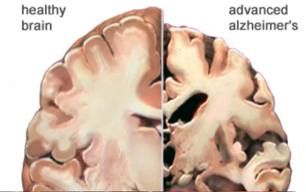

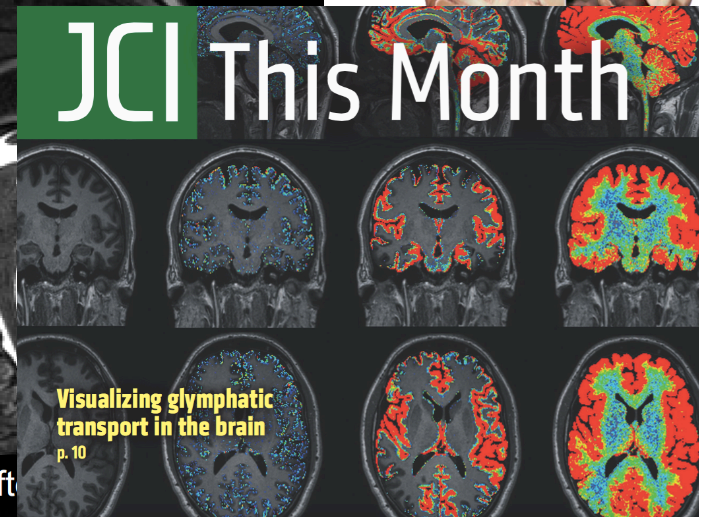

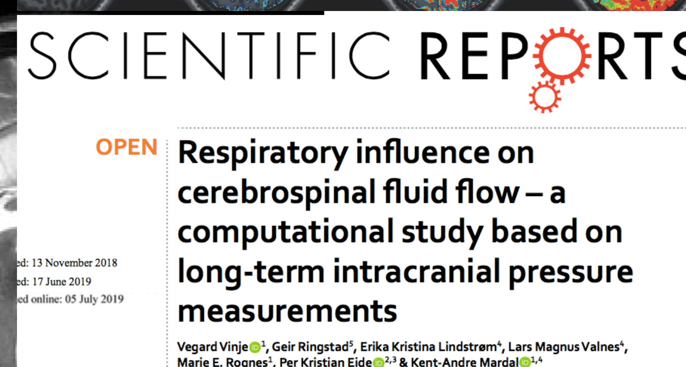

SCIENTIFIC REPORTS

OPEN

Respiratory influence on cerebrospinal fluid flow – a computational study based on long-term intracranial pressure measurements

ed: 13 November 2018
ed: 17 June 2019
ed online: 05 July 2019

Vegard Vinje[1], Geir Ringstad[5], Erika Kristina Lindstrøm[4], Lars Magnus Valnes[4], Marie E. Rognes[1], Per Kristian Eide[2,3] & Kent-Andre Mardal[1,4]

With Lars Magnus Valnes, Geir Ringstad, Per Kristian Eide

Roadmap for model development (?)

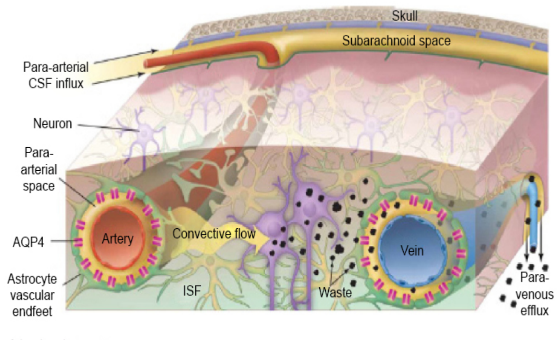

Take into account:
- poroelasticity
- complex, realistic geometries
- multiscale/multiphysics

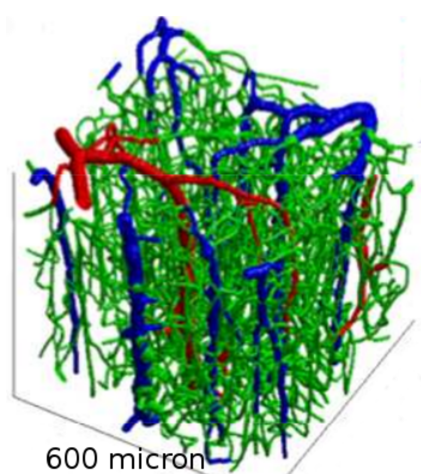

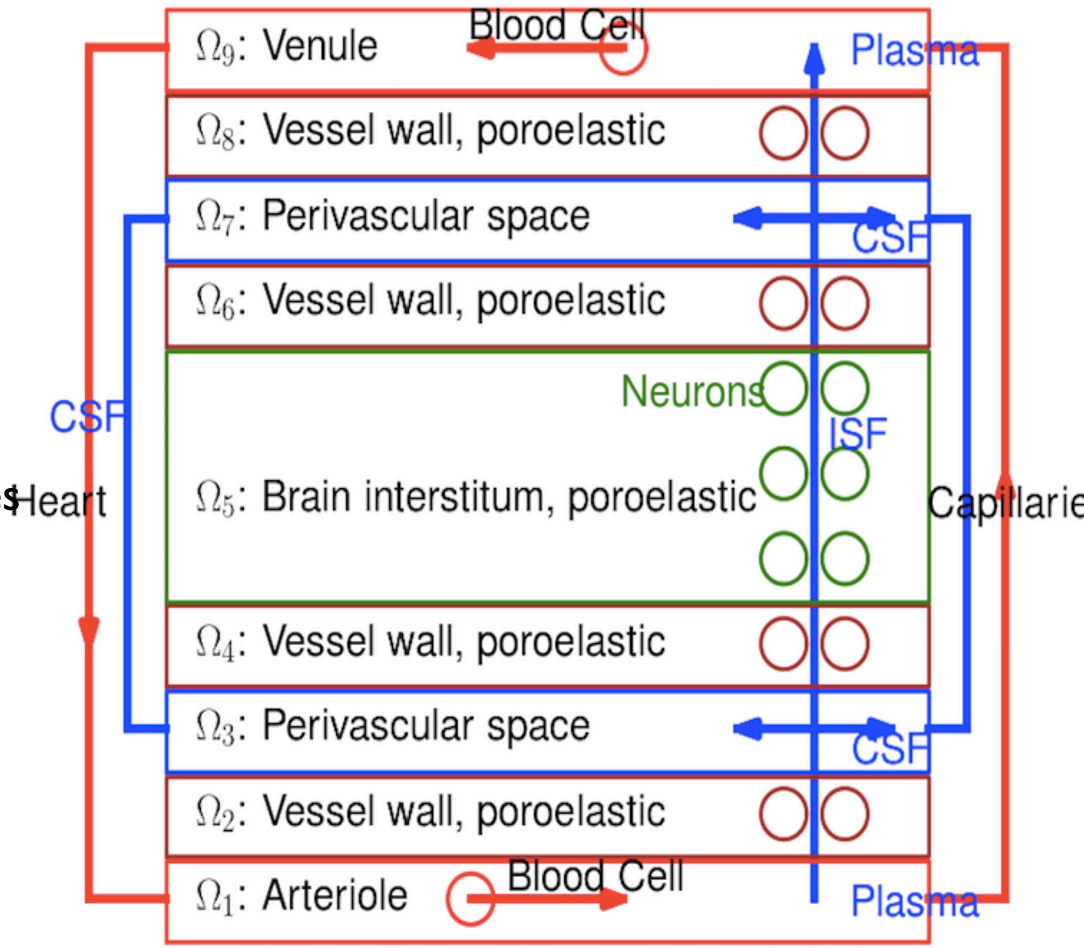

Requirements for the new models

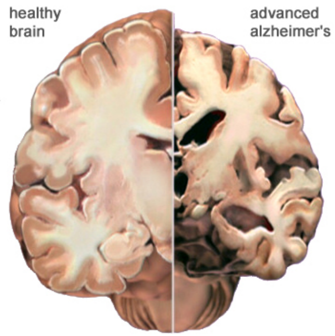

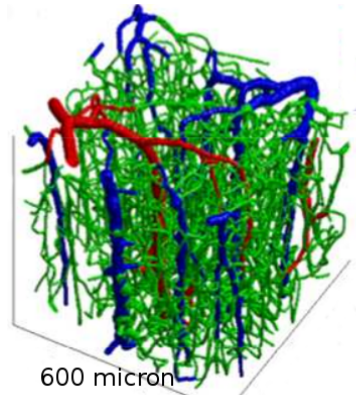

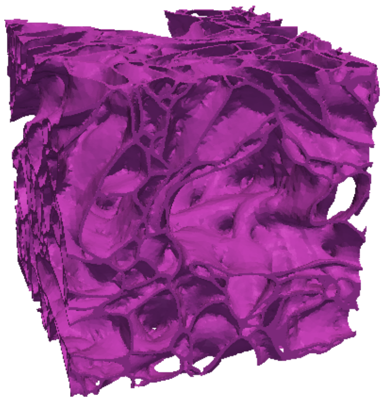

Features of the new modeling:

- geometry is complex at all interesting scales: HPC needed
- poroelasticity has not yet been taken into account
- the problem is a multiscale/multiphysics problem and the dynamics is slow

Main tool for designing efficient algorithms: Operator preconditioning

- Explain concepts of operator preconditioning in the context of coupled problems (viscous – porous flow)
- The need for fractional derivatives
- Extend to 3D-1D problems

Operator preconditioning in a nutshell

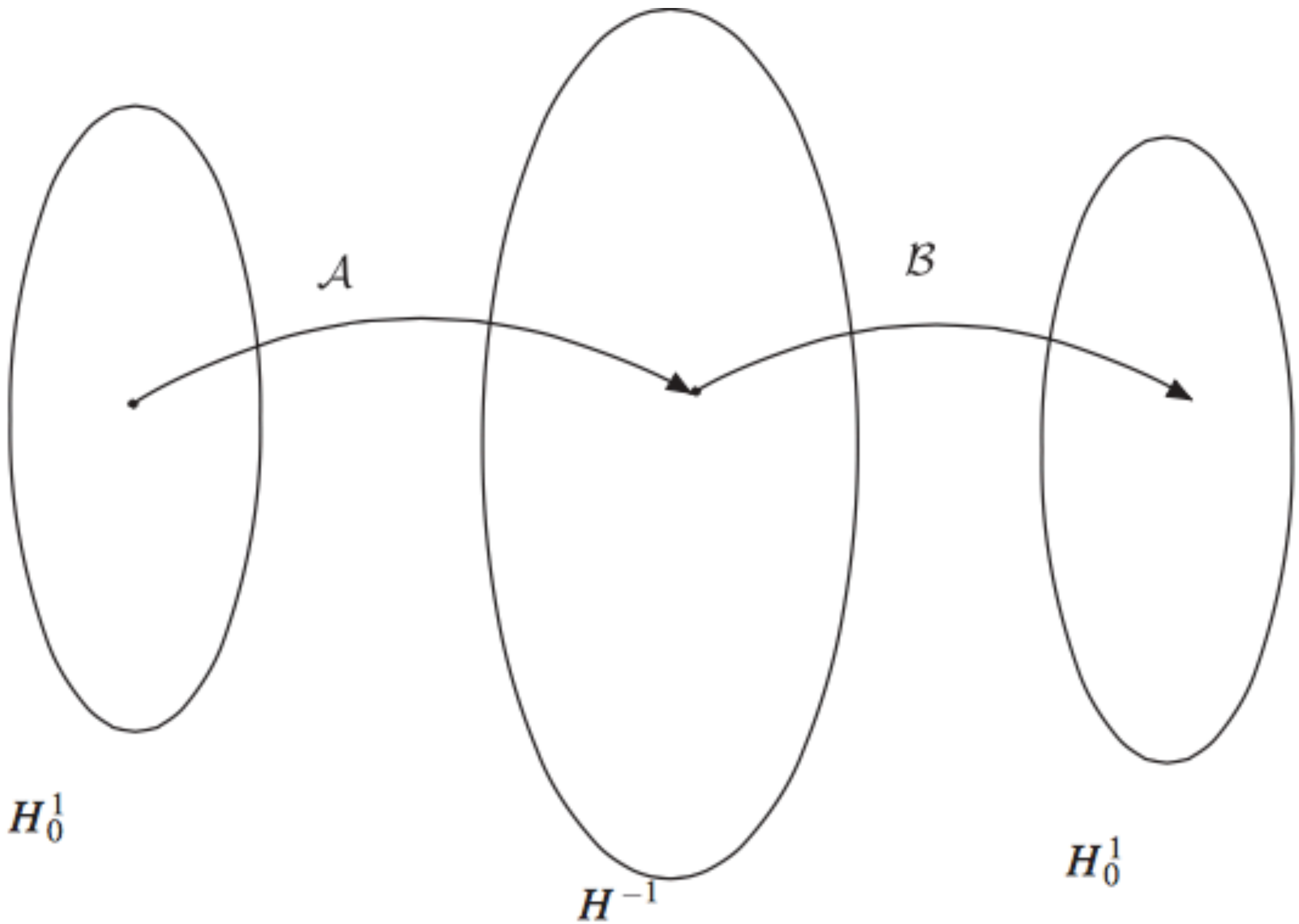

Mardal KA, Winther R. Preconditioning discretizations of systems of partial differential equations. Numerical Linear Algebra with Applications. 2011 Jan;18(1):1-40

Coupling of viscous and porous flow

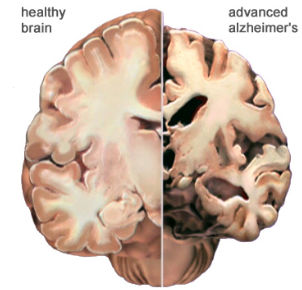

$$
\begin{aligned}
\mu \Delta \mathbf{u}_f - \nabla p_f &= 0 \text{ on } \Omega_f, \\
\nabla \cdot \mathbf{u}_f &= 0 \text{ on } \Omega_f, \\
\frac{\mu}{\kappa} \mathbf{u}_p - \Delta p_p &= 0 \text{ on } \Omega_p, \\
\nabla \cdot \mathbf{u}_p &= 0 \text{ on } \Omega_p, \\
\mathbf{u}_f \cdot \mathbf{n} &= \mathbf{u}_p \cdot \mathbf{n} \text{ on } \Gamma, \\
-\mu \frac{\partial \mathbf{u}_f}{\partial \mathbf{n}} \cdot \mathbf{n} + p_f &= p_p \text{ on } \Gamma, \\
-\mu \frac{\partial \mathbf{u}_f}{\partial \mathbf{n}} \cdot \mathbf{t} - D \mathbf{u}_f \cdot \mathbf{t} &= 0 \text{ on } \Gamma.
\end{aligned}
$$

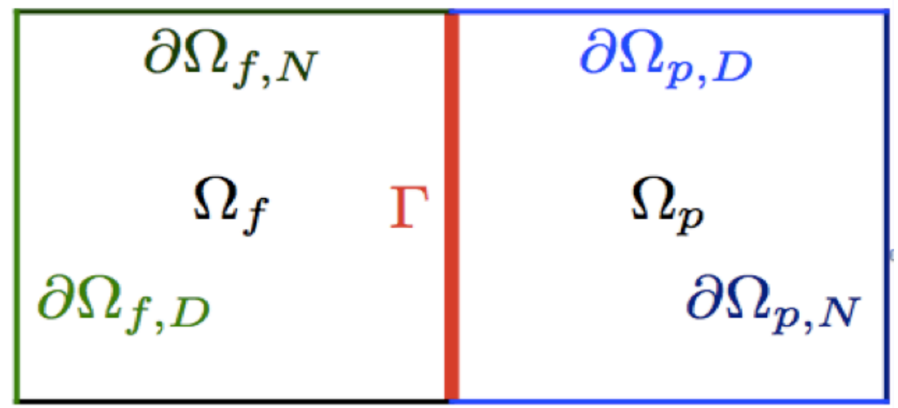

FIGURE 1. Schematic domain of Darcy-Stokes problem. Dirichlet conditions shown in green/blue, and interface in red.

Joint work with Karl Erik Holter and Miro Kuchta

Well-posedness, error estimates already done:

W. J. Layton, F. Schieweck, and I. Yotov, Coupling fluid flow with porous media flow, SIAM Journal on Numerical Analysis, 40 (2002)

J. Galvis and M. Sarkis, Non-matching mortar discretization analysis for the coupling Stokes-Darcy equations, Electron. Trans. Numer. Anal, 26 (2007),

Stokes problem – wellposedness is well known

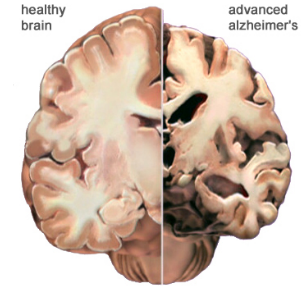

$$
\begin{aligned}
\Delta \mathbf{u} - \nabla p &= \mathbf{f} && \text{in } \Omega \\
\nabla \cdot \mathbf{u} &= 0 && \text{in } \Omega \\
\mathbf{u} &= 0 && \text{on } \partial\Omega
\end{aligned}
$$

$$\rightarrow \mathbf{u} \in H_0^1, p \in L_0^2$$

Stokes problem weighted by viscosity is not much different

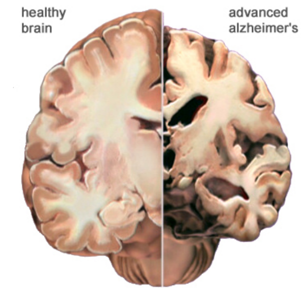

$$
\begin{aligned}
\Delta \mathbf{u} - \nabla p &= \mathbf{f} \quad \text{in } \Omega \\
\nabla \cdot \mathbf{u} &= 0 \quad \text{in } \Omega \\
\mathbf{u} &= 0 \quad \text{on } \partial\Omega
\end{aligned}
$$

$$\rightarrow \mathbf{u} \in H_0^1, p \in L_0^2$$

$$
\begin{aligned}
\mu\Delta \mathbf{u} - \nabla p &= \mathbf{f} \quad \text{in } \Omega \\
\nabla \cdot \mathbf{u} &= 0 \quad \text{in } \Omega \\
\mathbf{u} &= 0 \quad \text{on } \partial\Omega
\end{aligned}
$$

$$\rightarrow \mathbf{u} \in \mu^{1/2} H_0^1, p \in \mu^{-1/2} L_0^2$$

1

Stokes problem (some details about the weighted wellposedness)

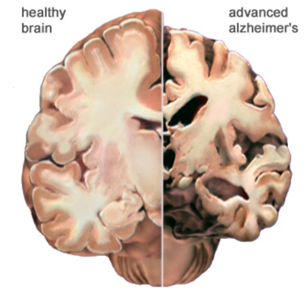

$$\|\mathbf{u}\|_{\mu^{1/2}H_0^1} = \left(\int_\Omega \mu\,(\nabla \mathbf{u})^2 dx\right)^{1/2}$$

$$\|p\|_{\mu^{-1/2}L_0^2} = \left(\int_\Omega \frac{1}{\mu} p^2 dx\right)^{1/2}$$

$$\int_\Omega \mu \nabla \mathbf{u} : \nabla \mathbf{v} dx = \int_\Omega \mu^{1/2} \nabla \mathbf{u} : \mu^{1/2} \nabla \mathbf{v} dx$$
$$\leq \|\mathbf{u}\|_{\mu^{1/2}H_0^1} \|\mathbf{v}\|_{\mu^{1/2}H_0^1}$$

$$\int_\Omega \nabla \cdot \mathbf{u}\, q dx = \int_\Omega (\mu^{1/2} \nabla \cdot \mathbf{u})\, \mu^{-1/2} q) dx$$
$$\leq \|\mathbf{u}\|_{\mu^{1/2}H_0^1} \|p\|_{\mu^{-1/2}L_0^2}$$

Darcy Problem well-posedness with permeability parameter is similar

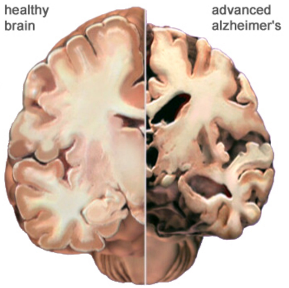

$$\frac{1}{K}\mathbf{u} - \nabla p = \mathbf{f} \quad \text{in } \Omega$$
$$\nabla \cdot \mathbf{u} = g \quad \text{in } \Omega$$

$$\rightarrow \mathbf{u} \in K^{-1/2}\mathbf{H}_0(\text{div}), p \in K^{1/2}L_0^2$$

$$\|\mathbf{u}\|_{K^{-1/2}\mathbf{H}(\text{div})} = (\int_\Omega \frac{1}{K}(\nabla \mathbf{u})^2 + \frac{1}{K}(\nabla \cdot \mathbf{u})^2 dx)^{1/2}$$
$$\|p\|_{K^{1/2}L_0^2} = (\int_\Omega K\, p^2 dx)^{1/2}$$

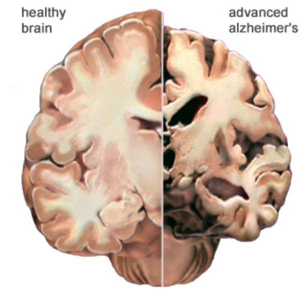

Coupling of viscous and porous flow

$$
\begin{aligned}
\mu\Delta \mathbf{u}_f - \nabla p_f &= 0 \text{ on } \Omega_f,\\
\nabla\cdot\mathbf{u}_f &= 0 \text{ on } \Omega_f,\\
\frac{\mu}{\kappa}\mathbf{u}_p - \Delta p_p &= 0 \text{ on } \Omega_p,\\
\nabla\cdot\mathbf{u}_p &= 0 \text{ on } \Omega_p,\\
\mathbf{u}_f\cdot\mathbf{n} &= \mathbf{u}_p\cdot\mathbf{n} \text{ on } \Gamma,\\
-\mu\frac{\partial\mathbf{u}_f}{\partial\mathbf{n}}\cdot\mathbf{n} + p_f &= p_p \text{ on } \Gamma,\\
-\mu\frac{\partial\mathbf{u}_f}{\partial\mathbf{n}}\cdot\mathbf{t} - D\mathbf{u}_f\cdot\mathbf{t} &= 0 \text{ on } \Gamma.
\end{aligned}
$$

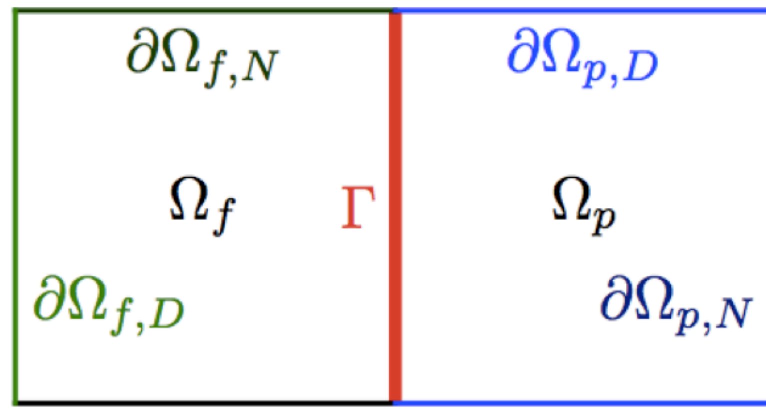

FIGURE 1. Schematic domain of Darcy-Stokes problem. Dirichlet conditions shown in green/blue, and interface in red.

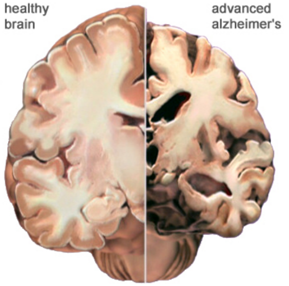

What is happening on the interface?

$$T(\mu^{1/2}H^1) = \mu^{1/2}H^{1/2}$$

$$T_n(K^{-1/2}\mathbf{H}(\mathrm{div})) = K^{-1/2}H^{-1/2}$$

$$\mu^{1/2}H^{1/2} \ni \mathbf{u}_f \cdot \mathbf{n} = \mathbf{u}_p \cdot \mathbf{n} \in K^{-1/2}H^{-1/2} \text{ on } \Gamma$$

$$(T_n \mathbf{u}_f - T_n \mathbf{u}_p, q) = 0, \forall q$$

What is happening on the interface?

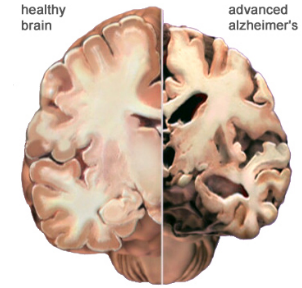

$$T(\mu^{1/2}H^1) = \mu^{1/2}H^{1/2}$$

$$T_n(K^{-1/2}\mathbf{H}(\mathrm{div})) = K^{-1/2}H^{-1/2}$$

$$\mu^{1/2}H^{1/2} \ni \mathbf{u}_f\cdot\mathbf{n} = \mathbf{u}_p\cdot\mathbf{n} \in K^{-1/2}H^{-1/2} \text{ on } \Gamma$$

$$(T_n\mathbf{u}_f - T_n\mathbf{u}_p, q) = 0, \forall q$$

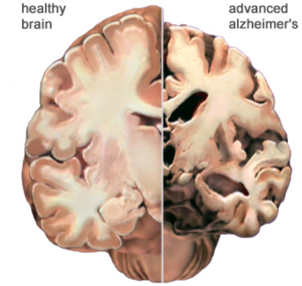

What is happening on the interface?

$$T(\mu^{1/2}H^1) = \mu^{1/2}H^{1/2}$$

$$T_n(K^{-1/2}\mathbf{H}(\mathrm{div})) = K^{-1/2}H^{-1/2}$$

$$\mu^{1/2}H^{1/2} \ni \mathbf{u}_f \cdot \mathbf{n} = \mathbf{u}_p \cdot \mathbf{n} \in K^{-1/2}H^{-1/2} \text{ on } \Gamma$$

$$(T_n\mathbf{u}_f - T_n\mathbf{u}_p, q) = 0, \forall q$$

$$T_n\mathbf{u}_f - T_n\mathbf{u}_p \in \mu^{1/2}H^{1/2}(\Gamma) + K^{-1/2}H^{-1/2}(\Gamma)$$

What is happening on the interface?

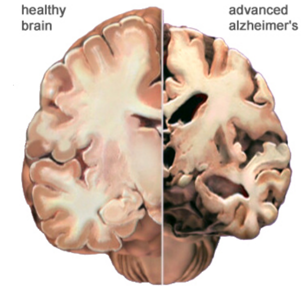

$$(T_n \mathbf{u}_f - T_n \mathbf{u}_p, q) = 0, \forall q$$

$$T_n \mathbf{u}_f - T_n \mathbf{u}_p \in \mu^{1/2} H^{1/2}(\Gamma) + K^{-1/2} H^{-1/2}(\Gamma)$$

$$q \in \mu^{-1/2} H^{-1/2}(\Gamma) \cap K^{1/2} H^{1/2}(\Gamma)$$

What happens on the interface II ?

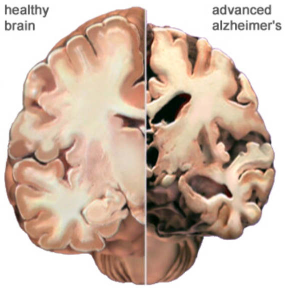

$$(T_n \mathbf{u}_f - T_n \mathbf{u}_p, q) = 0, \forall q$$

$$T_n \mathbf{u}_f - T_n \mathbf{u}_p \in \mu^{1/2} H^{1/2}(\Gamma) + K^{-1/2} H^{-1/2}(\Gamma)$$

$$q \in \mu^{-1/2} H^{-1/2}(\Gamma) \cap K^{1/2} H^{1/2}(\Gamma)$$

The sum of two Hilbert spaces X and Y is a Hilbert space denoted by X+Y
And its dual is the intersection of the dual spaces!

A preconditioner for the Darcy-Stokes problem (robust in all parameters)

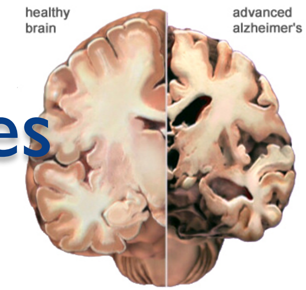

$$\mathcal{A} = \left(\begin{array}{cc|cc} -\mu\Delta & & -\nabla & & T_n' \\ & -1/K & & -\nabla & T_n' \\ \hline \nabla\cdot & & & & \\ & \nabla\cdot & & & \\ T_n & T_n & & & \end{array}\right) \begin{pmatrix} \mathbf{u}_f \\ \mathbf{u}_p \\ p_f \\ p_p \\ q \end{pmatrix} = \dots$$

$$\mathcal{B} = \left(\begin{array}{cc|ccc} -\mu\Delta & & & & \\ & \frac{1}{K}(I - \nabla\nabla\cdot) & & & \\ \hline & & \frac{1}{\mu} & & \\ & & & K & \\ & & & & \frac{1}{\mu}(-\Delta)^{-1/2} + K(-\Delta)^{1/2} \end{array}\right)^{-1}$$

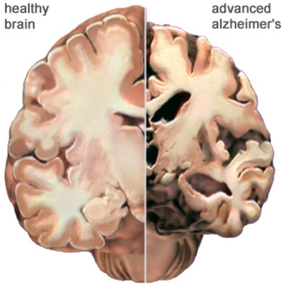

Iteration counts….

α_{BJS}	μ	K	h				
1	1	1	38	38	36	36	36
		10^{-2}	41	39	39	37	37
		10^{-4}	40	40	41	41	40
		10^{-6}	36	36	35	35	36
		10^{-8}	31	31	31	31	30
	10^{-2}	1.0	44	43	42	41	40
		10^{-2}	42	43	45	45	43
		10^{-4}	38	38	39	41	41
		10^{-6}	34	34	34	34	35
		10^{-8}	29	29	29	29	27
	10^{-4}	1.0	52	53	55	55	55
		10^{-2}	48	49	50	52	52
		10^{-4}	42	44	45	47	47
		10^{-6}	38	38	39	39	41
		10^{-8}	34	34	34	34	35
	10^{-6}	1.0	52	53	56	56	58
		10^{-2}	52	53	54	56	56
		10^{-4}	50	50	50	50	52
		10^{-6}	42	44	45	47	48
		10^{-8}	38	38	39	39	41
	10^{-8}	1.0	52	55	56	56	58
		10^{-2}	52	55	56	56	58
		10^{-4}	52	54	55	56	56
		10^{-6}	50	50	50	50	52
		10^{-8}	42	44	45	47	48

MinRes with an appropriate preconditioner

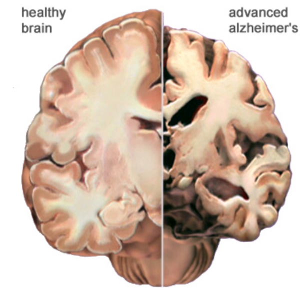

Final comment: boundary conditions for the Lagrange multiplier at the interface

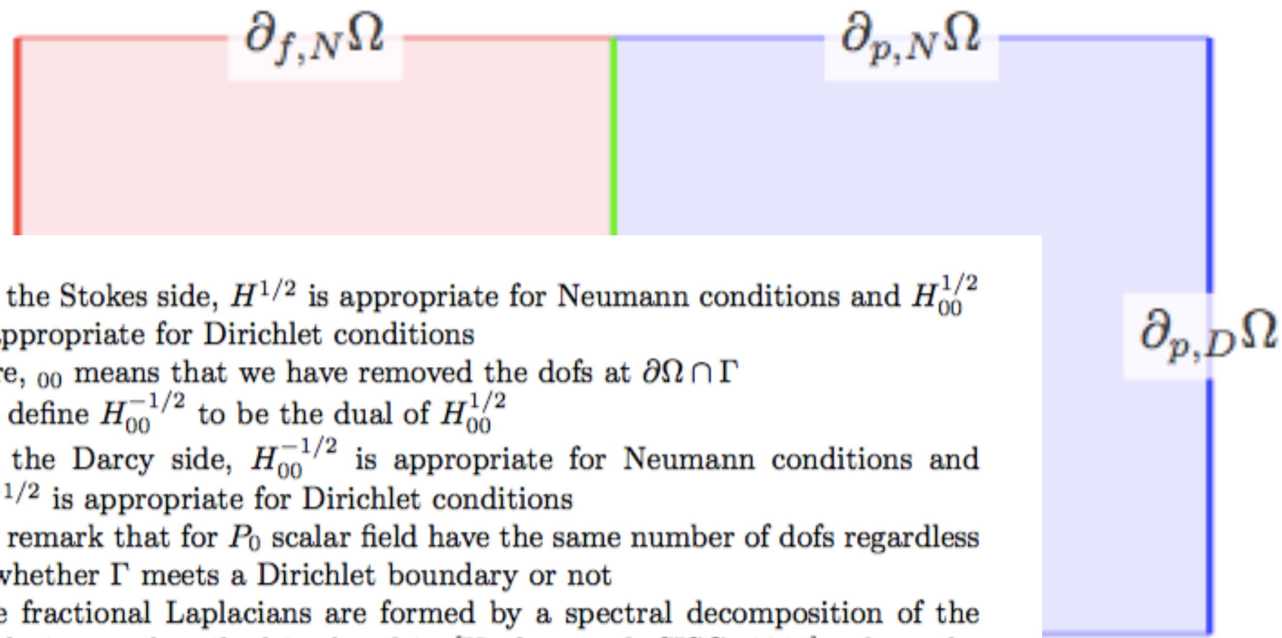

- On the Stokes side, $H^{1/2}$ is appropriate for Neumann conditions and $H^{1/2}_{00}$ is appropriate for Dirichlet conditions
- Here, $_{00}$ means that we have removed the dofs at $\partial\Omega \cap \Gamma$
- We define $H^{-1/2}_{00}$ to be the dual of $H^{1/2}_{00}$
- On the Darcy side, $H^{-1/2}_{00}$ is appropriate for Neumann conditions and $H^{-1/2}$ is appropriate for Dirichlet conditions
- We remark that for P_0 scalar field have the same number of dofs regardless of whether Γ meets a Dirichlet boundary or not
- The fractional Laplacians are formed by a spectral decomposition of the Laplacian as described in detail in [Kuchta et.al, SISC, 2016], where the Laplacian on piecewise constant field Q_h is defined as

$$(-\Delta p_h, q_h) = \sum_{E_I} \int_{E_I} \{\{h\}\}^{-1} [\![p]\!][\![q]\!] ds + \sum_{E_D} \int_{E_D} h^{-1} pq ds \quad p_h, q_h \in Q_h$$

where E_I is the set of internal facets of the mesh, while E_D is the set of facets associated with the Dirichlet boundary. Operators $[\![]\!]$ and $\{\{\}\}$ are the standard jump and average operators. Note that for operator $(-\Delta + I)^{-1/2}$ the set E_D is empty.

blem. Setting $\Gamma \cap$

Fractional Problems

- They show up at the interface in multi-physics/multi-scale problems
- Let us therefore consider fast solvers for:

$$(-\Delta)^s u = f$$

There has been a tremendous effort to discretize fractional Laplacians, but not so much about solving them

We have looked into how they can be solved with multilevel algorithms

Fractional Problems

- They show up at the interface in multi-physics/multi-scale problems
- Let us therefore consider fast solvers for:

$$(-\Delta)^s u = f$$

There has been a treme
but not so much about s

We have looked into ho

SIAM J. SCI. COMPUT.
Vol. 41, No. 2, pp. A948–A972

MULTIGRID METHODS FOR DISCRETE FRACTIONAL SOBOLEV SPACES*

TRYGVE BÆRLAND†, MIROSLAV KUCHTA†, AND KENT-ANDRE MARDAL†

Abstract. Coupled multiphysics problems often give rise to interface conditions naturally formulated in fractional Sobolev spaces. Here, both positive and negative fractionality are common. When designing efficient solvers for discretizations of such problems it would therefore be useful to have a preconditioner for the fractional Laplacian. In this work, we develop an additive multigrid preconditioner for the fractional Laplacian with positive fractionality and show a uniform bound on the condition number. For the case of negative fractionality, we reuse the preconditioner developed for the positive fractionality and left-right multiply a regular Laplacian with a preconditioner with positive fractionality to obtain the desired negative fractionality. Implementational issues are outlined in detail as the differences between the discrete operators and their corresponding matrices must

Vessels in a (0.6mm)^3 cube: 3D-1D coupled problem

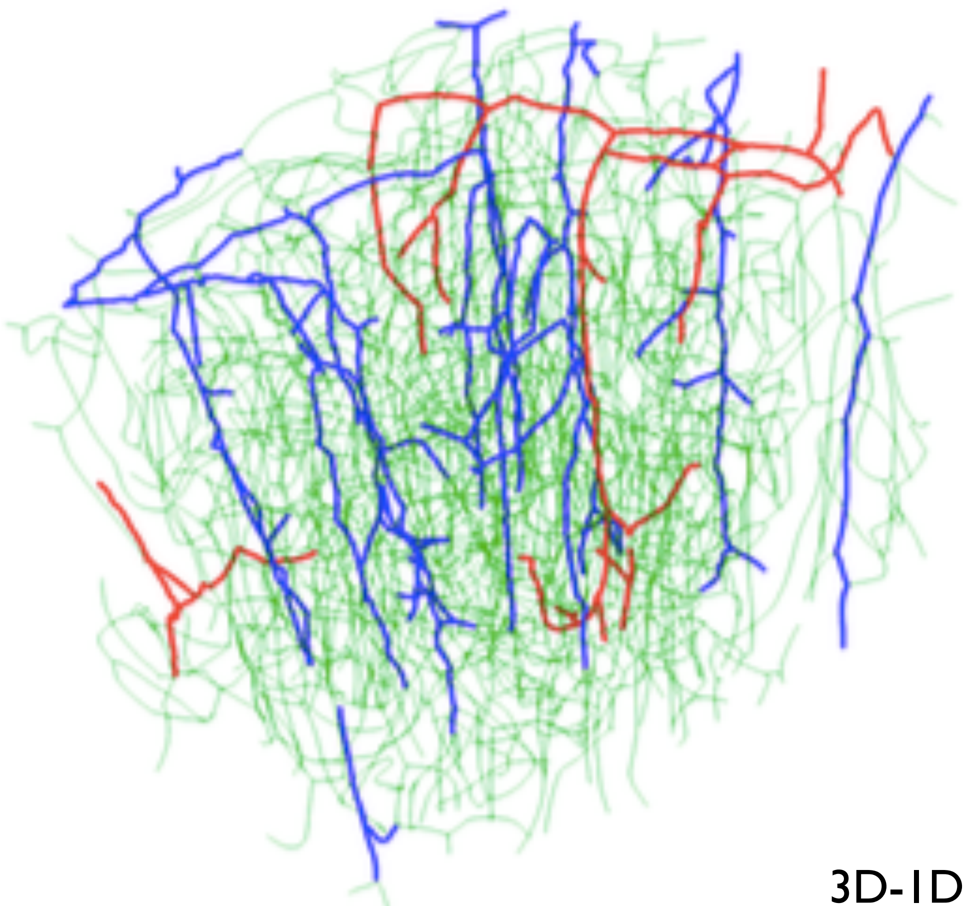

Boas, David A., et al. *Neuroimage* 40.3 (2008): 1116-1129.

3D-1D couplings:
D´Angelo, Quarteroni, Zunino: weighted spaces with distance functions

Simple test example 2D-1D problem

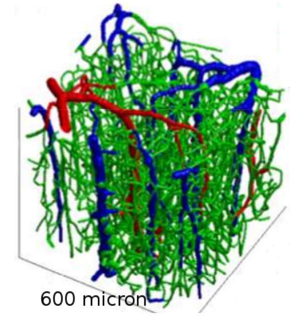

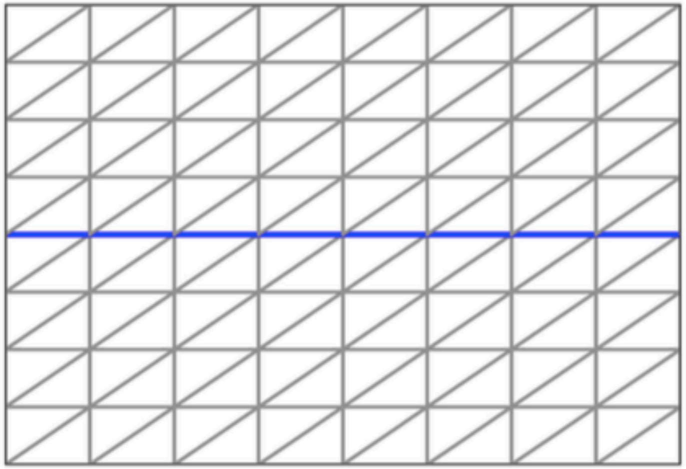

- Strong form

$$
\begin{aligned}
-\Delta u_1 &= f_1 && \text{in } \Omega \subset \mathbb{R}^2 \\
-u_2'' &= f_2 && \text{on } \Gamma = \{(x(s), y(s)) \in \Omega, s = [s_0, s_1]\} \\
\epsilon u_1 &= u_2 && \text{on } \Gamma
\end{aligned}
$$

2D-1D weak form

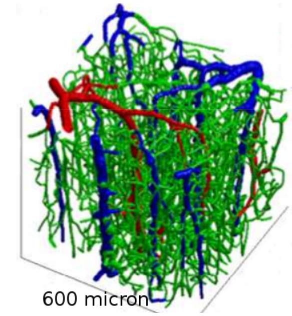

- Strong form

$$
\begin{aligned}
-\Delta u_1 &= f_1 && \text{in } \Omega \subset \mathbb{R}^2 \\
-u_2'' &= f_2 && \text{on } \Gamma = \{(x(s), y(s)) \in \Omega, s = [s_0, s_1]\} \\
\epsilon u_1 &= u_2 && \text{on } \Gamma \\
u_1 &= 0 && \text{on } \partial\Omega \\
u_2 &= 0 && \text{on } \partial\Gamma
\end{aligned}
$$

- Weak form using Lagrange multipliers. Find $u_1 \in V_1 := H_0^1 \in (\Omega)$, $u_2 \in V_2 := H_0^1(\Gamma)$, $p \in Q := H^{-1/2}(\Gamma)$:

$$
\begin{aligned}
(\nabla u_1, \nabla v_1)_\Omega + \langle p, \epsilon T v_1 \rangle &= (f_1, v_1) \\
(u_2', v_2')_\Gamma - \langle p, v_2 \rangle &= (f_2, v_2) \\
\langle q, \epsilon T u_1 - u_2 \rangle &= 0
\end{aligned}
$$

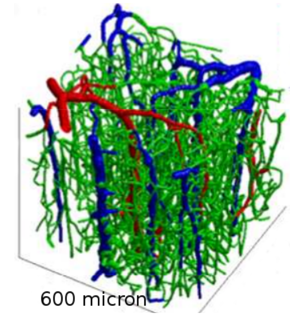

2D-1D Preconditioner

The original problem was

$$\mathcal{A} = \begin{bmatrix} -\Delta_\Omega & 0 & \epsilon T^* \\ 0 & -\Delta_\Gamma & I \\ \epsilon T & I & 0 \end{bmatrix} \begin{bmatrix} u \\ v \\ p \end{bmatrix} = \begin{bmatrix} f \\ g \\ 0 \end{bmatrix}$$

an appropriate preconditioner would then be

$$\mathcal{B} = \begin{bmatrix} -\Delta_\Omega & 0 & 0 \\ 0 & -\Delta_\Gamma & 0 \\ 0 & 0 & \epsilon^2(-\Delta_\Gamma^{-1/2}) + -\Delta_\Gamma^{-1} \end{bmatrix}^{-1}$$

- Robust preconditioner requires parameter-dependent spaces

$$V_1 = H_0^1(\Omega),\, V_2 = H_0^1(\Gamma),\, Q = \frac{1}{\epsilon}H^{-1/2}(\Gamma) \cap H^{-1}(\Gamma)$$

The preconditioner is good

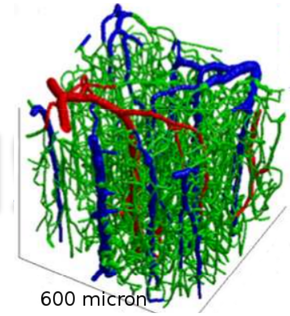

Table: Condition numbers

n_{3D}	n_{1D}	$\log_{10} \epsilon$						
		−3	−2	−1	0	1	2	3
99	9	2.655	2.969	4.786	6.979	7.328	7.357	7.360
323	17	2.698	3.323	5.966	7.597	7.697	7.715	7.717
1155	33	2.778	3.905	7.031	7.882	7.818	7.816	7.816
4355	65	2.932	4.769	7.830	8.016	7.855	7.843	7.843
16899	129	3.217	5.857	8.343	8.081	7.868	7.854	7.852
66563	257	3.710	6.964	8.637	8.113	7.872	7.856	7.855

Kuchta, Miroslav, et al. "Preconditioners for saddle point systems with trace constraints coupling 2d and 1d domains."
SIAM Journal on Scientific Computing 38.6 (2016):

3D-1D problem

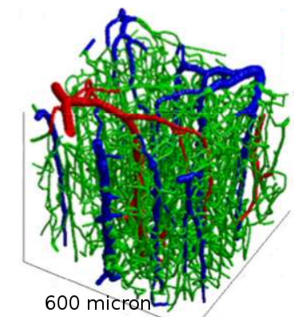

The original problem was

$$\mathcal{A} = \begin{bmatrix} -\Delta_\Omega & 0 & \epsilon T^* \\ 0 & -\Delta_\Gamma & I \\ \epsilon T & I & 0 \end{bmatrix} \begin{bmatrix} u \\ v \\ p \end{bmatrix} = \begin{bmatrix} f \\ g \\ 0 \end{bmatrix}$$

an appropriate preconditioner would then be

$$\mathcal{B} = \begin{bmatrix} -\Delta_\Omega & 0 & 0 \\ 0 & -\Delta_\Gamma & 0 \\ 0 & 0 & \epsilon^2(-\Delta_\Gamma^{-0.14}) + -\Delta_\Gamma^{-1} \end{bmatrix}^{-1}$$

- Robust preconditioner requires parameter-dependent spaces

$$V_1 = H_0^1(\Omega),\ V_2 = H_0^1(\Gamma),\ Q = \frac{1}{\epsilon} H^{-0.14}(\Gamma) \cap H^{-1}(\Gamma)$$

Kuchta, M., Mardal, K.A., & Mortensen, M. (2019). Preconditioning trace coupled 3d-1d systems using fractional Laplacian.
Numerical Methods for Partial Differential Equations, 35(1)

Simple multiscale 3d-1d models of viscous – porous couping

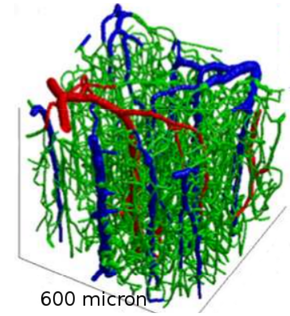

Vasculature resolved as a three-dimensional structure

$$
\begin{aligned}
-\nabla \cdot (\kappa \nabla u) &= f \quad \text{in } \Omega, \\
-\nabla \cdot (\hat{\kappa} \nabla \hat{u}) &= \hat{f} \quad \text{in } \hat{\Omega}, \\
u - \hat{u} &= g \quad \text{on } \Gamma, \\
\kappa \nabla u \cdot n - \hat{\kappa} \nabla \hat{u} \cdot n &= h \quad \text{on } \Gamma.
\end{aligned}
$$

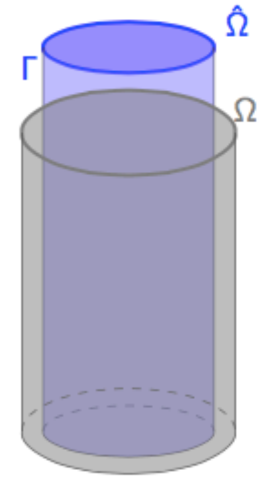

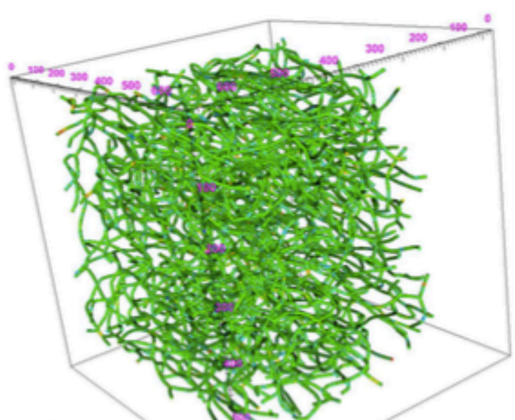

Impractical for real geometries

Joint work with Federica Laurino, Miroslav Kuchta and Paolo Zunino

Multiscale 3d-1d model by dimensional reduction

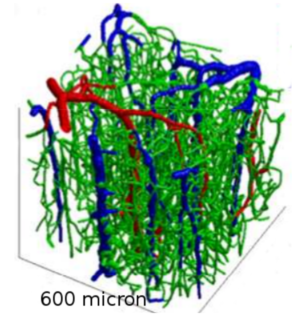

Current models lead non-typical elliptic operators

$$(\Pi_R u)(y) = (2\pi R)^{-1} \int_{\mathcal{C}_R(y)} u \circ C_R \mathrm{d}l, R \ll \mathrm{diam}(\Omega)$$

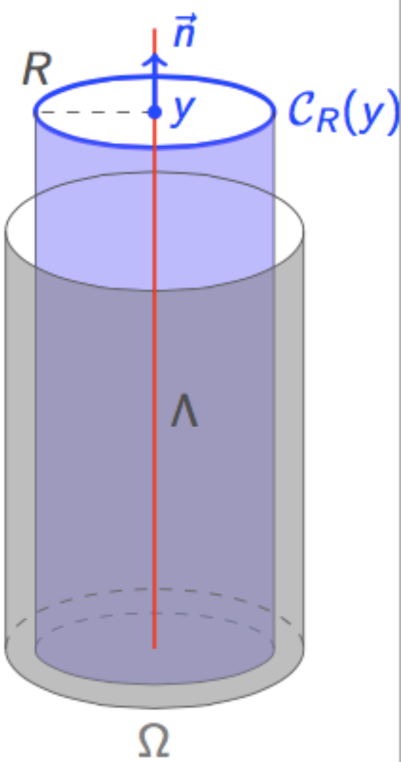

- D'Angelo, Quarteroni: assymetric continuous problem $\mathcal{A} : V \mapsto \hat{V}'$

$$\mathcal{A} = \begin{pmatrix} -\kappa\Delta_\Omega & -T' \\ -\beta\Pi_R & -R^2\hat{\kappa}\Delta_\Lambda \end{pmatrix}$$

with $V = H^1_\alpha(\Omega) \times H^1(\Gamma)$, $\hat{V} = H^1_{-\alpha}(\Omega) \times H^1(\Gamma)$

- Cerrroni, Laurino, Zunnino: symmetric problem $\mathcal{A} : V \mapsto V'$

$$\mathcal{A} = \begin{pmatrix} -\kappa\Delta_\Omega + \Pi_R'\Pi_R & -\beta\Pi_R' \\ -\Pi_R & -R^2\hat{\kappa}\Delta_\Lambda \end{pmatrix}$$

with $V = H^1(\Omega) \times H^1(\Gamma)$

Can we use common black-box preconditioners?

Lagrange multiplier 3d-1d formulation

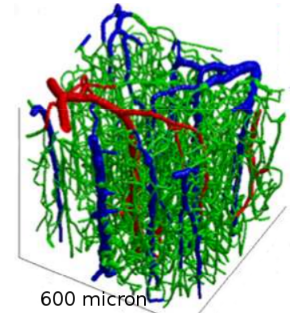

Offers possibly more flexible coupling

Consider $\mathcal{A} : H^1(\Omega) \times H^1(\Lambda) \times Q$

$$\mathcal{A} = \begin{pmatrix} -\kappa\Delta_\Omega & & \Pi' \\ & -R^2\hat{\kappa}\Delta_\Lambda & -\hat{\Pi}' \\ \Pi & -\hat{\Pi} & \end{pmatrix}$$

Two options for the Lagrange multiplier space

- Q defined on Λ
- Q defined in *virtual* coupling surface Γ

We wish to construct block-diagonal preconditioners

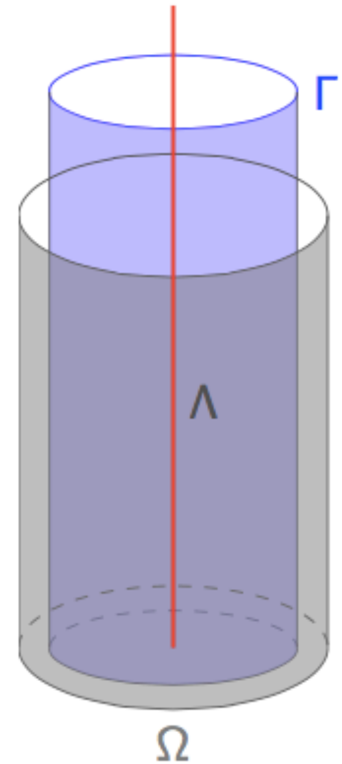

Formulation with line multiplier, conforming P1

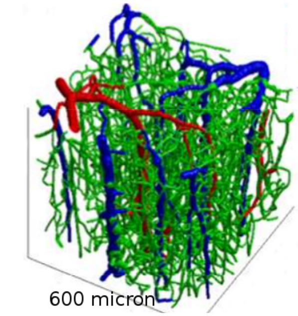

Riesz map preconditioner I

$$\mathcal{B} = \begin{pmatrix} -\Delta_\Omega & & \\ & -R^2\Delta_\Lambda & \\ & & (-\Delta_\Gamma)^{-1/2} \end{pmatrix}^{-1}$$

h	2^{-2}	2^{-3}	2^{-4}	2^{-5}
cond($\mathcal{BA}$)	40.5	40.6	40.6	40.6

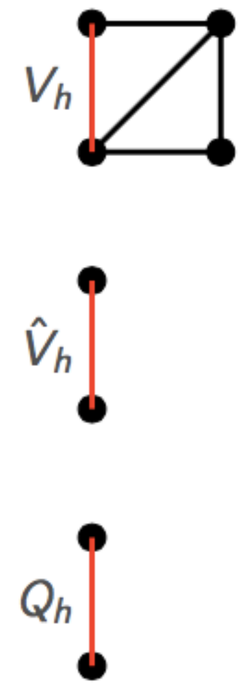

Schur complement of $\mathcal{A}$ is R dependent, $\Pi = \Pi_R$, $\hat{\Pi} = I$

$$R^2(\Pi)(-\Delta_\Omega)^{-1}(\Pi)' + (\hat{\Pi})(-\Delta_\Lambda)^{-1}(\hat{\Pi})'$$

R-robust preconditioner

$$\mathcal{B} = \begin{pmatrix} -\Delta_\Omega & & \\ & -R^2\Delta_\Lambda & \\ & & R^2(-\Delta_\Gamma)^{-1/2} + (-\Delta_\Gamma)^{-1} \end{pmatrix}^{-1}$$

α	h			
	2^{-2}	2^{-3}	2^{-4}	2^{-5}
10^{-1}	4.5162	4.5201	4.5608	4.6189
10^{-2}	4.5314	4.5366	4.5574	4.6137
10^{-3}	4.5311	4.5312	4.5315	4.5328

Nonconforming line multiplier, P1-P1-P0 elements

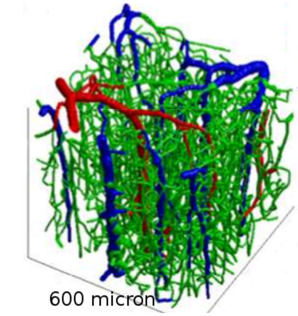

Stabilized FEM formulation

$$\mathcal{A} = \begin{pmatrix} -\kappa\Delta_\Omega & & \Pi' \\ & -R^2\hat{\kappa}\Delta_\Lambda & -\hat{\Pi}' \\ \Pi & -\hat{\Pi} & -h^3\Delta_{\Gamma,h} \end{pmatrix} \qquad \langle p, -\Delta_{\Gamma,h} q\rangle = \sum \{\{h\}\}^{-1} [\![p]\!][\![q]\!]$$

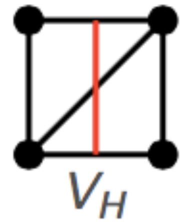

Conforming-case preconditioner with stabilization term

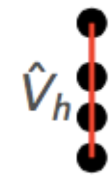

α	h			
	2^{-2}	2^{-3}	2^{-4}	2^{-5}
10^{-1}	4.5316	4.5319	4.5289	4.5506
10^{-2}	4.5412	4.5399	4.5364	4.5337
10^{-3}	4.5413	4.5310	4.5364	4.5439

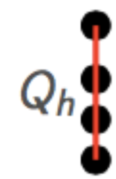

Formulation with surface multiplier, conforming P1

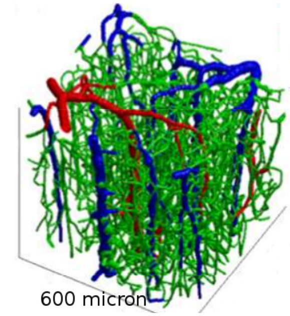

Coupling via

- $\Pi = T$ (standard 3d-2d trace)
- $\hat{\Pi}$ extension operator $\Lambda \to \Gamma$

Riesz map preconditioner I

$$\mathcal{B} = \begin{pmatrix} -\Delta_\Omega & & \\ & -R^2\Delta_\Lambda & \\ & & (-\Delta_\Gamma)^{-1/2} \end{pmatrix}^{-1}$$

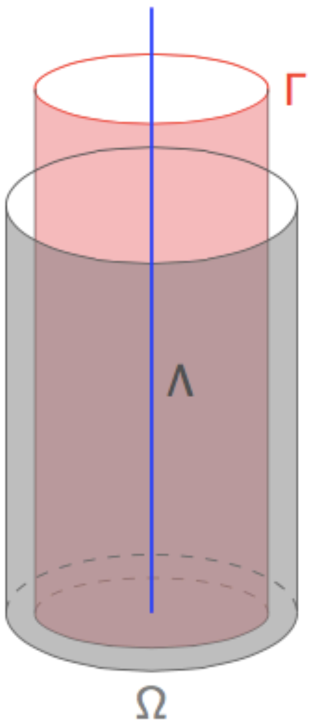

At the moment only h-robust

h	2^{-2}	2^{-3}	2^{-4}	2^{-5}
cond($\mathcal{BA}$)	27.4	27.5	27.6	27.6

Fractional preconditioner computationally expensive

Conclusion

- Alzheimer´s disease and the glymphatic system are in need of new modeling
- Waste clearance, porous media flow seems a powerful framework
- Numbers don´t add up, permeability and fluid velocities seem to low: A lot of open questions!
- Multiscale (3D-1D) and multi-physics approach is warrented
- Operator preconditioning is a powerful way of unraveling the underlying structures and create efficient algorithms

Further readings, acknowledgement

Trygve Bærland	*Anders Dale*	***Per Kristian Eide***	***Karl Erik Holter***
Miro Kuchta	*Erlend Nagelhus*	***Federica Laurino***	*John Lee*
Klas Pettersen	*Eleonora Piersanti*	***Geir Ringstad***	***Paolo Zunino***
Marie Rognes	***Lars Magnus Valnes***	*Vegard Vinje*	*Ragnar Winther*

Holter, Kehlet, Devor, Sejnowskif, Dale, Omholt, Ottersen, Nagelhus, Mardal, Pettersen, Interstitial solute transport in 3D reconstructed neuropil: diffusion predominates, online in PNAS, 2017

Ringstad G, Valnes LM, Dale AM, Pripp AH, Vatnehol SA, Emblem KE, Mardal KA, Eide PK. Brain-wide glymphatic enhancement and clearance in humans assessed with MRI. JCI insight. 2018 Jul 12;3(13).

Bærland T, Kuchta M, Mardal KA. Multigrid Methods for Discrete Fractional Sobolev Spaces. SIAM Journal on Scientific Computing. 2019 Apr 2;41(2):A948-72.

Mardal KA, Winther R. Preconditioning discretizations of systems of partial differential equations. Numerical Linear Algebra with Applications. 2011 Jan 1;18(1):1-40.

Kuchta M, Mardal KA, Mortensen M. Preconditioning trace coupled 3d-1d systems using fractional Laplacian. Numerical Methods for Partial Differential Equations. 2019 Jan;35(1):375-93

Holter KE, Kuchta M, Mardal KA. Robust preconditioning for coupled Stokes-Darcy problems with the Darcy problem in primal form. arXiv preprint arXiv:2001.05529.

Holter, K. E., Kuchta, M., & Mardal, K. A. (2020). Robust preconditioning of monolithically coupled multiphysics problems. arXiv preprint arXiv:2001.05527